Revised Version

DESY-04-036
ZU-TH-02/04

DESY-04-036
ZU-TH 02/04
March 2004

An Analysis of the Time-Dependent CP Asymmetry in $B \to \pi\pi$ Decays in the Standard Model

Ahmed Ali

Theory Group, Deutsches Elektronen-Synchrotron DESY, D-22603 Hamburg, FRG. [a]

Enrico Lunghi

Institut für Theoretische Physik, Universität Zürich, CH-8057 Zürich, Switzerland. [b]

Alexander Ya. Parkhomenko

Institut für Theoretische Physik, Universität Bern, CH-3012 Bern, Switzerland. [c] [d]

April 5, 2004

Abstract

Measurements of the time-dependent CP asymmetry in the decay $B^0_d(t) \to \pi^+\pi^-$ and its charge conjugate by the BELLE and BABAR collaborations currently yield $C^{+-}_{\pi\pi} = -0.46 \pm 0.13$ and $S^{+-}_{\pi\pi} = -0.74 \pm 0.16$, characterizing the direct and mixing-induced CP asymmetries, respectively. We study the implication of these measurements on the CKM phenomenology taking into account the available information in the quark mixing sector. Our analysis leads to the results that the ratio $|P_c/T_c|$ involving the QCD-penguin and tree amplitudes and the related strong phase difference $\delta_c = \delta^P_c - \delta^T_c$ in the $B^0_d/\bar{B}^0_d \to \pi^+\pi^-$ decays are quite substantial. Using the isospin symmetry to constrain $|P_c/T_c|$ and $\cos(2\theta)$, where 2θ parameterizes the penguin-induced contribution, we present a fit of the current data including the measurements of $S^{+-}_{\pi\pi}$ and $C^{+-}_{\pi\pi}$. Our best-fits yield: $\alpha = 92°$, $\beta = 24°$, $\gamma = 64°$, $|P_c/T_c| = 0.77$, and $\delta_c = -43°$. At 68% C.L., the ranges are: $81° \le \alpha \le 103°$, $21.9° \le \beta \le 25.5°$, $54° \le \gamma \le 75°$, $0.43 \le |P_c/T_c| \le 1.35$ and $-64° \le \delta_c \le -29°$. Currently *en vogue* dynamical approaches to estimate the hadronic matrix elements in $B \to \pi\pi$ decays do not provide a good fit of the current data.

[a] E-mail: ahmed.ali@desy.de
[b] E-mail: lunghi@physik.unizh.ch
[c] E-mail: parkh@itp.unibe.ch
[d] On leave of absence from Department of Theoretical Physics, Yaroslavl State University, Sovietskaya 14, 150000 Yaroslavl, Russia.

1 Introduction

Precise measurement of CP-violation in B-meson decays is the principal goal of experiments at the current electron-positron B-factories, KEK-B and SLAC-B, and at the hadron colliders, Tevatron and LHC. In the standard model (SM), the source of CP violation is the Kobayashi-Maskawa phase [1] which resides in the Cabibbo-Kobayashi-Maskawa (CKM) matrix [1,2]. In the Wolfenstein parameterization [3] of the CKM matrix, characterized by the parameters λ, A, ρ and η, CP violation is related to a non-zero value of the parameter η. Of particular importance in the analysis of CP violation in the B-meson sector is the following unitarity relation:

$$V_{ud}V_{ub}^* + V_{cd}V_{cb}^* + V_{td}V_{tb}^* = 0, \tag{1}$$

which is a triangle relation in the complex $\bar{\rho} - \bar{\eta}$ plane, depicted in Fig. 1. Here, $\bar{\rho} = (1 - \lambda^2/2)\,\rho$ and $\bar{\eta} = (1 - \lambda^2/2)\,\eta$ are the perturbatively improved Wolfenstein parameters [4]. The sides of this triangle, called R_b and R_t, are defined as

$$R_b \equiv \sqrt{\bar{\rho}^2 + \bar{\eta}^2}, \qquad R_t \equiv \sqrt{(1-\bar{\rho})^2 + \bar{\eta}^2}, \tag{2}$$

and its three inner angles have their usual definitions:

$$\alpha \equiv \arg\left(-\frac{V_{tb}^* V_{td}}{V_{ub}^* V_{ud}}\right), \quad \beta \equiv \arg\left(-\frac{V_{cb}^* V_{cd}}{V_{tb}^* V_{td}}\right), \quad \gamma \equiv \arg\left(-\frac{V_{ub}^* V_{ud}}{V_{cb}^* V_{cd}}\right). \tag{3}$$

The BELLE collaboration uses a different notation for these angles: $\phi_1 = \beta$, $\phi_2 = \alpha$, and $\phi_3 = \gamma$. We recall that among the CKM matrix elements above V_{ub} and V_{td} have sizable imaginary parts, and hence all three angles α, β and γ are sizable. Of these, the phase β has already been well measured using the time-dependent CP asymmetries in the $B \to J/\psi K_S$ and related decays, yielding [5]:

$$\sin(2\beta) = \sin(2\phi_1) = 0.736 \pm 0.049, \qquad \beta = \phi_1 = 23.8^\circ \pm 2.0^\circ. \tag{4}$$

The current thrust [6] of the two B-factory experiments – BABAR and BELLE – is now on the measurements of the other two angles α (or ϕ_2) and γ (or ϕ_3). Of these, the weak phase α will be measured through the CP violation in the $B \to \pi\pi$, $B \to \rho\pi$ and $B \to \rho\rho$ decays. To eliminate the hadronic uncertainties in the determination of α, an isospin analysis of these final states (as well as an angular analysis in the $\rho\rho$ case) will be necessary [7]. To carry out the isospin analysis in $B \to \pi\pi$ decays, one needs to know the three amplitudes A^{+-}, A^{00} and A^{+0}, corresponding to the $B_d^0 \to \pi^+\pi^-$, $B_d^0 \to \pi^0\pi^0$ and $B^+ \to \pi^+\pi^0$ decays, respectively, and their charge conjugates $\bar{A}^{ij}$. At present, the only missing pieces in the current data are A^{00} and $\bar{A}^{00}$ – the amplitudes of the $B_d^0 \to \pi^0\pi^0$ and $\bar{B}_d^0 \to \pi^0\pi^0$ decays, respectively – though the measured charge conjugate averaged branching ratio [8] $\mathcal{B}(B^0/\overline{B^0} \to \pi^0\pi^0)$ provides an information on the sum $|\bar{A}^{00}|^2 + |A^{00}|^2$. Hence, a model-independent isospin analysis of the $B \to \pi\pi$ decays can not be carried out at present from the branching ratios alone.

In addition to the measurements of the branching ratios in the $B \to \pi\pi$ decays, the time-dependent CP asymmetries in the $B_d^0(t)/\bar{B}_d^0(t) \to \pi^+\pi^-$ and $B_d^0(t)/\bar{B}_d^0(t) \to \pi^0\pi^0$ decays will greatly help in pinning down the weak phase α. We shall concentrate here on the CP-asymmetry in the decay $B_d^0 \to \pi^+\pi^-$, which is defined as follows:

$$\begin{aligned} a_{\pi\pi}^{+-}(t) &\equiv \frac{\Gamma[\bar{B}_d^0(t) \to \pi^+\pi^-] - \Gamma[B_d^0(t) \to \pi^+\pi^-]}{\Gamma[\bar{B}_d^0(t) \to \pi^+\pi^-] + \Gamma[B_d^0(t) \to \pi^+\pi^-]} \\ &= S_{\pi\pi}^{+-} \sin(\Delta M_B\, t) - C_{\pi\pi}^{+-} \cos(\Delta M_B\, t), \end{aligned} \tag{5}$$

where ΔM_B is the mass difference in the $B_d^0 - \bar{B}_d^0$ system which is already well measured [9], and $C_{\pi\pi}^{+-}$ and $S_{\pi\pi}^{+-}$ are the direct and mixing-induced CP asymmetry parameters, respectively. In the notation used by the BELLE collaboration [10], $C_{\pi\pi}^{+-}$ is replaced by $A_{\pi\pi}^{+-}$, where $A_{\pi\pi}^{+-} = -C_{\pi\pi}^{+-}$.

The BABAR [11,6] and BELLE [10] measurements were summarized last summer at the Lepton-Photon 2003 conference, yielding the world averages [6]: $S_{\pi\pi}^{+-} = -0.58 \pm 0.20$ and $C_{\pi\pi}^{+-} = -0.38 \pm 0.16$. However,

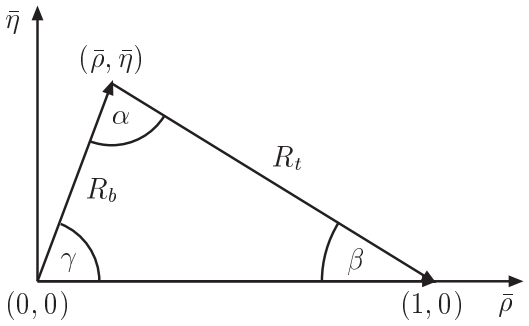

Figure 1. The unitarity triangle with the unit base in the $\bar{\rho}-\bar{\eta}$ plane. The two sides R_b and R_t and the angles α (ϕ_2), β (ϕ_1) and γ (ϕ_3) are defined in Eqs. (2) and (3), respectively.

a significant disagreement between the two measurements existed and the confidence level that the two are compatible with each other, in particular in the measurement of $S^{+-}_{\pi\pi}$, was rather low (4.7% C.L.). Recently, the BELLE collaboration have updated their results for $S^{+-}_{\pi\pi}$ and $A^{+-}_{\pi\pi}$ by including more data. The current BELLE measurements [12] (based on 140 fb^{-1} data) together with the updated BABAR results [6] (based on 113 fb^{-1} data) of these quantities are as follows:

$$S^{+-}_{\pi\pi} = \begin{cases} -0.40 \pm 0.22 \pm 0.03 \text{ (BABAR)} \\ -1.00 \pm 0.21 \pm 0.07 \text{ (BELLE)} \end{cases}, \quad C^{+-}_{\pi\pi} = \begin{cases} -0.19 \pm 0.19 \pm 0.05 \text{ (BABAR)} \\ -0.58 \pm 0.15 \pm 0.07 \text{ (BELLE)} \end{cases}. \tag{6}$$

They have been averaged by the Heavy Flavor Averaging Group [HFAG] to yield [9]

$$S^{+-}_{\pi\pi} = -0.74 \pm 0.16, \qquad C^{+-}_{\pi\pi} = -0.46 \pm 0.13, \tag{7}$$

and correspond to 4.6 and 3.5 standard deviation measurements from null results, respectively. It is also reassuring to note that the BELLE and BABAR measurements are now closer to each other than was the case at the Lepton-Photon 2003 conference, having now a scale factor [e] of 1.7 in $S^{+-}_{\pi\pi}$ and 1.4 in $C^{+-}_{\pi\pi}$. Significant updates of the BABAR and BELLE results in the $B \to \pi\pi$ decays are awaited later this year which will further firm up these measurements.

As can be judged from the results in (7), current measurements of $S^{+-}_{\pi\pi}$ and $C^{+-}_{\pi\pi}$ have already reached a significant level and invite a theoretical analysis leading to a determination of the unitarity triangle angles α and hence also γ. The importance of these measurements for the CKM phenomenology has been long anticipated and discussed at great length in the literature [13,14,15,16,17,18,19]. Our analysis taking into account the updated $B \to \pi\pi$ data has many features which it shares conceptually with the cited literature and we shall compare our results with the ones obtained in the more recent works [17,18]. A prerequisite to carry out such an analysis is to get model-independent bounds on the non-perturbative dynamical quantities $|P_c/T_c|$ and $\delta_c = \delta^P_c - \delta^T_c$, involving the so-called QCD-penguin P_c and color-allowed tree T_c topologies. Here, the subscripts denote that we are using the c-convention of Gronau and Rosner [20] in choosing the independent CKM factors in the analysis of the $B \to \pi\pi$ decays. Discussions of the ambiguities in the penguin amplitudes have also been presented earlier [21,22,23]. Our approach makes use of the isospin-based bounds on the ratio $|P_c/T_c|$ and δ_c in the analysis of the data in the $B \to \pi\pi$ sector and we show how to incorporate these bounds in the analysis of the unitarity triangle in the SM.

There are essentially three parameters $|P_c/T_c|$, δ_c and α [the weak phase β is already well measured, see Eq. (4)], which can not be determined from the measurements of just two quantities $S^{+-}_{\pi\pi}$ and $C^{+-}_{\pi\pi}$. However, correlations and bounds on these parameters can be obtained which have been presented by

[e] We thank the Heavy Flavor Averaging Group and, in particular, Andreas Höcker, for providing us the updated averages and the scale factors.

the BELLE collaboration based on their data [10,12]. In the first part of our paper we undertake a similar analysis of the combined BABAR and BELLE data and work out the best-fit values and bounds on the parameters δ_c and $|P_c/T_c|$. As our analysis is performed within the SM, we allow the phase β to vary in the experimental range and restrict the range of α from the indirect unitarity-triangle (UT) analysis, which we have taken from the CKM fitter [24] and another recent fit of the CKM parameters [25]. We first show in this paper that the current data on $S^{+-}_{\pi\pi}$ and $C^{+-}_{\pi\pi}$ restricts the two strong interaction parameters δ_c and $|P_c/T_c|$. This information is already helpful in providing some discrimination on various competing approaches incorporating QCD dynamics in these decays. Conversely, restricting the allowed range of $|P_c/T_c|$ from the current dynamical models, data on $S^{+-}_{\pi\pi}$ and $C^{+-}_{\pi\pi}$ allows to put constraints on α. This has been done by the BELLE collaboration [12], yielding at 95.5% C.L. $90^\circ \leq \phi_2 \leq 146^\circ$ for $0.15 \leq |P_c/T_c| \leq 0.45$ and $\sin(2\phi_1) = 0.746$. However, due to the restrictions on $|P_c/T_c|$, this remains a model-dependent enterprise.

Our analysis differs in this respect from the one carried out by the BELLE collaboration. Instead of restricting $|P_c/T_c|$ by a survey of models, we use the isospin symmetry to restrict the range of $|P_c/T_c|$ and δ_c. To do this, we harness all the current data available on the branching ratios for $B^0_d \to \pi^+\pi^-$, $B^+ \to \pi^+\pi^0$ and $B^0_d \to \pi^0\pi^0$ decays (and their charge conjugates), $S^{+-}_{\pi\pi}$ and $C^{+-}_{\pi\pi}$, and study a number of correlations, in particular $|P_c/T_c|$ vs. $\cos(2\theta)$, where θ is a penguin-related angle which is connected with the relative phase between the amplitudes A^{+-} and $\tilde{A}^{+-}$ (see Fig. 2). It is well known that the isospin symmetry can be used to put a lower bound on $\cos(2\theta)$, as first pointed out by Grossman and Quinn [26]. Subsequently, the Grossman-Quinn bound was improved by Charles [27], who derived in addition a new bound involving the $B^0_d \to \pi^0\pi^0$ and $B^0_d \to \pi^+\pi^-$ decay modes. Based on the observation that the $B \to \pi\pi$ amplitudes can be represented, using the isospin symmetry, as two (closed) triangles which have a common base, Gronau et. al [28] derived an improved lower bound on $\cos(2\theta)$ – the Gronau-London-Sinha-Sinha (GLSS) bound. We illustrate this bound numerically using current data and the constraints that it implies in the $|P_c/T_c| - \cos(2\theta)$ plane for both the $\theta > 0$ and $\theta < 0$ cases, varying γ in a large range $25^\circ \leq \gamma \leq 75^\circ$, which adequately covers the present range of this angle allowed by the UT fits at 95% C.L. Lest it be misunderstood, we emphasize that our final results for the CKM parameters and the dynamical quantities make no restrictions on the range of γ, whose value will be returned together with those of the other quantities by our CKM unitarity fits. The isospin-based lower bound on $\cos(2\theta)$, and hence an upper bound on $|\theta|$, is a model-independent constraint on the penguin contribution in the analysis of the data involving the measurements of $S^{+-}_{\pi\pi}$ and $C^{+-}_{\pi\pi}$.

There are yet other bounds based on the isospin symmetry in $B \to \pi\pi$ decays which lead to restrictions on γ. In particular, the Buchalla-Safir bound [30] on γ (and its various reincarnations discussed recently in the literature [31,19]) result from the correlations involving $\sin(2\beta)$, γ, $S^{+-}_{\pi\pi}$, and $C^{+-}_{\pi\pi}$. We have analyzed these bounds, but we find that they are not very useful at present as the current central values of $\sin(2\beta)$ and $-S^{+-}_{\pi\pi}$ almost coincide. For these bounds to be useful phenomenologically, the value of $-S^{+-}_{\pi\pi}$ has to come down substantially.

In the last part of our analysis, we study the impact of the $S^{+-}_{\pi\pi}$ and $C^{+-}_{\pi\pi}$ measurements on the profile of the unitarity triangle in a model-independent way. We first show that the quality of the UT fits is not modified by the inclusion of the data on $S^{+-}_{\pi\pi}$ and $C^{+-}_{\pi\pi}$, as the two additional parameters $|P_c/T_c|$ and δ_c, when varied in large regions, can always reproduce the central values of the $S^{+-}_{\pi\pi}$ and $C^{+-}_{\pi\pi}$ averages. We then implement the lower bound on $\cos(2\theta)$ in performing the fits of the unitarity triangle in the $\bar{\rho} - \bar{\eta}$ plane. The present bound $\cos(2\theta) > 0.27$ removes a small part of the otherwise allowed region of the unitarity triangle, but this constraint will become more significant in future as the errors on the $B \to \pi\pi$ branching ratios, $S^{+-}_{\pi\pi}$ and $C^{+-}_{\pi\pi}$ are reduced. The effects of the bound on $\cos(2\theta)$ are also shown on the correlations $\alpha - \gamma$ and $\cos(2\alpha) - \cos(2\beta)$. Working out the χ^2-distributions in the quantities α, $|P_c/T_c|$ and δ_c, we find that the current data prefers rather large values for the latter two quantities, with the minimum of the χ^2-distributions being at $|P_c/T_c| = 0.77$ and $\delta_c = -43^\circ$. The corresponding best-fit values of α and γ are $\alpha = 92^\circ$ and $\gamma = 64^\circ$. At 68% C.L., the ranges are: $81^\circ \leq \alpha \leq 103^\circ$, $21.9^\circ \leq \beta \leq 25.5^\circ$, $54^\circ \leq \gamma \leq 75^\circ$, $0.43 \leq |P_c/T_c| \leq 1.35$, and $-64^\circ \leq \delta_c \leq -29^\circ$. The bound on $\cos(2\theta)$

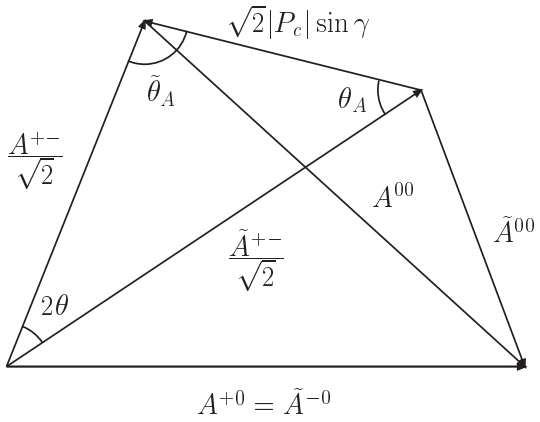

Figure 2. The isospin triangle for the $B \to \pi\pi$ decay amplitudes A^{ij} and the same for the phase-shifted charge-conjugate ones $\tilde{A}^{ij} = \mathrm{e}^{2i\,\gamma}\,\bar{A}^{ij}$ in the complex plane.

is very efficient in the exclusion of the large values of $|P_c/T_c|$ and $-\delta_c$. Their best-fit values are quite a bit larger than anticipated in most dynamical approaches. This feature has also been noted in earlier studies on the $B \to \pi\pi$ decays [13,17,18].

This paper is organized as follows: In section 2, we give the relations among the observables in the $B_d^0 \to \pi^+\pi^-$ decay and its charge conjugate, the CKM parameters and various dynamical quantities. Section 3 contains a review of several isospin-based bounds in the $B \to \pi\pi$ decays. In section 4, we report on the results of our numerical analysis of the time-dependent CP asymmetry in the $B_d^0/\bar{B}_d^0 \to \pi^+\pi^-$ decays, and in section 5 we show the results of the unitarity triangle fits, correlations involving the angles α, β and γ, and the dynamical quantities $|P_c/T_c|$ and δ_c, carried out in the context of the SM. We conclude with a summary and some remarks in section 6.

2 Relations among the Observables in the $B \to \pi\pi$ Decays, CKM Parameters and Dynamical Quantities

In this section we present the analytic formulae that we need to discuss the time-dependent CP asymmetry and the branching ratio in the $B_d^0 \to \pi^+\pi^-$ decay, and their relations with the CKM parameters and various dynamical quantities.

The amplitudes $A^{+-} \equiv A[B_d^0 \to \pi^+\pi^-]$ and its charge-conjugate $\bar{A}^{+-} \equiv A[\bar{B}_d^0 \to \pi^+\pi^-]$ can be written by using the Gronau-Rosner c-convention [20] as follows:

$$\begin{aligned} A^{+-} &= V_{ub}^* V_{ud}\, A_u^{+-} + V_{cb}^* V_{cd}\, A_c^{+-} + V_{tb}^* V_{td}\, A_t^{+-} \qquad (8)\\ &= V_{ub}^* V_{ud}\left(A_u^{+-} - A_t^{+-}\right) + V_{cb}^* V_{cd}\left(A_c^{+-} - A_t^{+-}\right)\\ &\equiv -\left(|T_c|\, e^{i\delta_c^T}\, e^{+i\gamma} + |P_c|\, e^{i\delta_c^P}\right),\\ \bar{A}^{+-} &= V_{ub} V_{ud}^*\left(A_u^{+-} - A_t^{+-}\right) + V_{cb} V_{cd}^*\left(A_c^{+-} - A_t^{+-}\right) \qquad (9)\\ &\equiv -\left(|T_c|\, e^{i\delta_c^T}\, e^{-i\gamma} + |P_c|\, e^{i\delta_c^P}\right). \end{aligned}$$

In getting the last expressions for the amplitudes the unitarity relation (1) has been used together with the phase convention $V_{ub} = |V_{ub}|\, e^{-i\gamma}$ for this CKM matrix element.

The phenomenon of the $B_d^0 - \bar{B}_d^0$ mixing modulates the time dependence of the decay amplitudes for

$B^0_d(t) \to \pi^+\pi^-$ and $\bar{B}^0_d(t) \to \pi^+\pi^-$:

$$\mathcal{A}^{+-}(t) = e^{-iM_B t} e^{-\Gamma t/2} \Bigg\{ \cos\frac{\Delta M_B t}{2} \left[\cosh\frac{\Delta\Gamma t}{4} - \lambda^{+-}_{\pi\pi} \sinh\frac{\Delta\Gamma t}{4} \right] + i \sin\frac{\Delta M_B t}{2} \left[\lambda^{+-}_{\pi\pi} \cosh\frac{\Delta\Gamma t}{4} - \sinh\frac{\Delta\Gamma t}{4} \right] \Bigg\} A^{+-}, \tag{10}$$

$$\bar{\mathcal{A}}^{+-}(t) = e^{-iM_B t} e^{-\Gamma t/2} \Bigg\{ \cos\frac{\Delta M_B t}{2} \left[\lambda^{+-}_{\pi\pi} \cosh\frac{\Delta\Gamma t}{4} - \sinh\frac{\Delta\Gamma t}{4} \right] + i \sin\frac{\Delta M_B t}{2} \left[\cosh\frac{\Delta\Gamma t}{4} - \lambda^{+-}_{\pi\pi} \sinh\frac{\Delta\Gamma t}{4} \right] \Bigg\} \frac{p}{q} A^{+-}. \tag{11}$$

Here, M_B and Γ are the average mass and decay width of the $B^0_d - \bar{B}^0_d$ system, and ΔM_B and $\Delta\Gamma$ are the the mass- and width- difference in the two mass eigenstates, respectively, $p/q \simeq V^*_{td}/V_{td} = e^{2i\beta}$ is the mixing parameter, and the quantity:

$$\lambda^{+-}_{\pi\pi} = \frac{q}{p}\frac{\bar{A}^{+-}}{A^{+-}} = e^{2i\alpha} \frac{1 + |P_c/T_c|\, e^{i\delta_c}\, e^{+i\gamma}}{1 + |P_c/T_c|\, e^{i\delta_c}\, e^{-i\gamma}} \equiv |\lambda^{+-}_{\pi\pi}|\, e^{2i\alpha_{\rm eff}}, \tag{12}$$

is introduced which encodes all the information about the CP asymmetry in this decay. Here, $\alpha_{\rm eff} = \alpha + \theta$, and θ is the penguin-pollution parameter shown in Fig. 2, which is connected with the relative phase between the amplitudes A^{+-} and $\bar{A}^{+-}$, $\Delta\phi^{+-} = 2(\gamma + \theta)$, and the relation $\alpha + \beta + \gamma = \pi$ has been used. Note that in the limit $P_c/T_c \to 0$, $\theta \to 0$ and $\alpha_{\rm eff} \to \alpha$.

The partial decay widths of the time-dependent $B^0_d(t) \to \pi^+\pi^-$ and $\bar{B}^0_d(t) \to \pi^+\pi^-$ decays are proportional, respectively, to [32]

$$|\mathcal{A}^{+-}(t)|^2 = e^{-\Gamma t}\, B^{+-}_{\pi\pi} \left[1 + C^{+-}_{\pi\pi} \cos(\Delta M_B t) - S^{+-}_{\pi\pi} \sin(\Delta M_B t) \right], \tag{13}$$

$$|\bar{\mathcal{A}}^{+-}(t)|^2 = e^{-\Gamma t}\, B^{+-}_{\pi\pi} \left[1 - C^{+-}_{\pi\pi} \cos(\Delta M_B t) + S^{+-}_{\pi\pi} \sin(\Delta M_B t) \right], \tag{14}$$

where $|p/q| = 1$ is used and the following quantities are introduced:

$$B^{+-}_{\pi\pi} = \frac{1}{2}\left[|A^{+-}|^2 + |\bar{A}^{+-}|^2 \right] = \frac{1}{2}\left[1 + |\lambda^{+-}_{\pi\pi}|^2 \right] |A^{+-}|^2, \tag{15}$$

$$C^{+-}_{\pi\pi} = \frac{|A^{+-}|^2 - |\bar{A}^{+-}|^2}{|A^{+-}|^2 + |\bar{A}^{+-}|^2} = \frac{1 - |\lambda^{+-}_{\pi\pi}|^2}{1 + |\lambda^{+-}_{\pi\pi}|^2}, \tag{16}$$

$$S^{+-}_{\pi\pi} = \frac{2\,{\rm Im}\left[(q/p)\bar{A}^{+-}(A^{+-})^* \right]}{|A^{+-}|^2 + |\bar{A}^{+-}|^2} = \frac{2\,{\rm Im}\,\lambda^{+-}_{\pi\pi}}{1 + |\lambda^{+-}_{\pi\pi}|^2} \equiv y^{+-}_{\pi\pi}\, \sin(2\alpha_{\rm eff}), \tag{17}$$

$$y^{+-}_{\pi\pi} = \frac{2\,|A^{+-}|\,|\bar{A}^{+-}|}{|A^{+-}|^2 + |\bar{A}^{+-}|^2} = \frac{2\,|\lambda^{+-}_{\pi\pi}|}{1 + |\lambda^{+-}_{\pi\pi}|^2}. \tag{18}$$

Using the expression for $\lambda^{+-}_{\pi\pi}$ given in Eq. (12), the above quantities can be rewritten in the following form:

$$B^{+-}_{\pi\pi} \equiv |T_c|^2\, R^{+-}_{\pi\pi} = |T_c|^2 + 2|P_c||T_c| \cos\delta_c \cos\gamma + |P_c|^2, \tag{19}$$

$$C^{+-}_{\pi\pi} = \frac{2}{R^{+-}_{\pi\pi}} \left| \frac{P_c}{T_c} \right| \sin\delta_c \sin\gamma, \tag{20}$$

$$S^{+-}_{\pi\pi} = \frac{1}{R^{+-}_{\pi\pi}} \left[\sin(2\alpha) - 2 \left| \frac{P_c}{T_c} \right| \cos\delta_c \sin(\alpha - \beta) - \left| \frac{P_c}{T_c} \right|^2 \sin(2\beta) \right], \tag{21}$$

$$y^{+-}_{\pi\pi} = \sqrt{1 - \left(C^{+-}_{\pi\pi} \right)^2}. \tag{22}$$

Making the back transformation, $|T_c|$, $|P_c|$ and δ_c can be expressed as follows:

$$|T_c|^2 = \frac{B^{+-}_{\pi\pi}}{1 - \cos(2\gamma)} \left[1 - y^{+-}_{\pi\pi} \cos(2\theta - 2\gamma) \right], \tag{23}$$

$$|P_c|^2 = \frac{B^{+-}_{\pi\pi}}{1-\cos(2\gamma)}\left[1 - y^{+-}_{\pi\pi}\,\cos(2\theta)\right], \tag{24}$$

$$\tan\delta_c = \frac{C^{+-}_{\pi\pi}\,\sin\gamma}{y^{+-}_{\pi\pi}\,\cos(2\theta-\gamma) - \cos\gamma}. \tag{25}$$

In the limit of neglecting the penguin contribution (i.e., $|P_c| \to 0$), the CP-asymmetry coefficient $C^{+-}_{\pi\pi}$ goes to zero (and $y^{+-}_{\pi\pi} \to 1$) as well as $\theta \to 0$, in agreement with Eq. (24). Also, in this limit, $B^{+-}_{\pi\pi} = |T_c|^2$, as in this case the branching ratio is completely defined by the tree contribution.

In terms of γ and θ, the penguin-to-tree ratio squared has the following expression:

$$r_c^2 \equiv \left|\frac{P_c}{T_c}\right|^2 = \frac{1 - y^{+-}_{\pi\pi}\,\cos(2\theta)}{1 - y^{+-}_{\pi\pi}\,\cos(2\theta-2\gamma)} = \frac{1 - y^{+-}_{\pi\pi}\,\cos(2\alpha_{\rm eff}-2\alpha)}{1 - y^{+-}_{\pi\pi}\,\cos(2\alpha_{\rm eff}+2\beta)}. \tag{26}$$

This relation constrains r_c in terms of $\cos(2\theta)$, given γ and $y^{+-}_{\pi\pi}$. It should be noted that for fixed values of $y^{+-}_{\pi\pi}$ and r_c, $\cos(2\gamma)$ varies in the range:

$$-1 \le \cos(2\gamma) \le \frac{1 - (C^{+-}_{\pi\pi})^2(1+r_c^4)/(2r_c^2)}{1-(C^{+-}_{\pi\pi})^2}. \tag{27}$$

It is easy to see that the upper limit of $\cos(2\gamma)$ is equal to 1 when $r_c = 1$, independent of $C^{+-}_{\pi\pi}$. For $r_c \neq 1$, the allowed range of $\cos(2\gamma)$ puts a constraint in the $r_c - C^{+-}_{\pi\pi}$ plane. Thus, the allowed domain of r_c is completely defined by the direct CP-asymmetry coefficient and, for negative $C^{+-}_{\pi\pi}$ (in accordance with the experimental data), it is given by

$$(r_c)_{\rm min,max} = -\frac{1 \pm \sqrt{1-(C^{+-}_{\pi\pi})^2}}{C^{+-}_{\pi\pi}}. \tag{28}$$

In particular, for the central experimental value $C^{+-}_{\pi\pi} = -0.46$, the allowed range of r_c is as follows:

$$0.244 \le r_c \le 4.104. \tag{29}$$

For the current experimental central value of $C^{+-}_{\pi\pi}$, and its $\pm 1\sigma$ limits, the dependence of the upper limit $\cos(2\gamma)|_{\rm UL}$ on the magnitude of the penguin-to-tree ratio is presented in Fig. 3. Decreasing the magnitude of $C^{+-}_{\pi\pi}$, the allowed region of r_c becomes wider. The expression for $\cos(2\theta)$ as a function of $y^{+-}_{\pi\pi}$, r_c and $\cos(2\gamma)$ is as follows:

$$\cos(2\theta) = \frac{(1-r_c^2)[1-r_c^2\cos(2\gamma)] \pm r_c^2\sqrt{[1-\cos^2(2\gamma)]\{2(y^{+-}_{\pi\pi})^2 r_c^2[1-\cos(2\gamma)] - (1-r_c^2)^2[1-(y^{+-}_{\pi\pi})^2]\}}}{y^{+-}_{\pi\pi}\{(1-r_c^2)^2 + 2r_c^2[1-\cos(2\gamma)]\}}. \tag{30}$$

3 Isospin-Based Bounds in $B \to \pi\pi$ Decays

With partial experimental information on $B \to \pi\pi$ decays available at present, it is of practical importance to get useful restrictions on the dynamical parameters at hand, r_c and δ_c. It is obvious from (25) and (26), that apart from $C^{+-}_{\pi\pi}$, which is measured from the time-dependent CP asymmetry, the angle 2θ plays a central role in constraining the dynamical parameters of interest. While 2θ will be determined eventually from the measurement of A^{00} and $\tilde{A}^{00}$ (see Fig. 2), this is not the case now. Instead, several bounds have been derived on $\cos(2\theta)$ using the isospin symmetry, which we review here. The first of these which we will work out numerically is the GLSS bound [28]:

$$\cos(2\theta) \ge \frac{(B^{+-}_{\pi\pi} + 2B^{+0}_{\pi\pi} - 2B^{00}_{\pi\pi})^2 - 4B^{+-}_{\pi\pi}B^{+0}_{\pi\pi}}{4y^{+-}_{\pi\pi}B^{+-}_{\pi\pi}B^{+0}_{\pi\pi}}, \tag{31}$$

where $B^{+0}_{\pi\pi}$ and $B^{00}_{\pi\pi}$ are the quantities constructed from the $B^+ \to \pi^+\pi^0$ and $B^0_d \to \pi^0\pi^0$ decay amplitudes in a similar way as in Eq. (15). It was also demonstrated by Gronau et. al [28] that this bound is

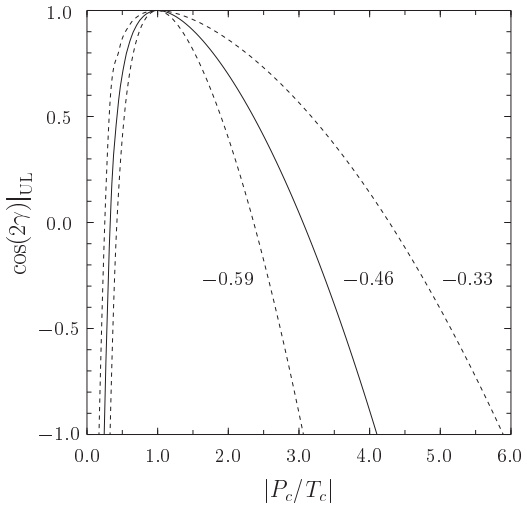

Figure 3. The dependence of the upper limit $\cos(2\gamma)_{\rm UL}$ on the ratio $|P_c/T_c|$ for $C^{+-}_{\pi\pi} = -0.46$ (the current central value), $C^{+-}_{\pi\pi} = -0.59$ and $C^{+-}_{\pi\pi} = -0.33$, which demarcate the $\pm 1\sigma$ experimental measurements.

stronger than both the Grossman-Quinn and Charles bounds. As a byproduct, a bound on the direct CP asymmetry $C^{00}_{\pi\pi}$ in the $B^0_d \to \pi^0\pi^0$ decay was also obtained by these authors [28]:

$$C^{00}_{\pi\pi} \geq C^{+-}_{\pi\pi}\, \frac{B^{+-}_{\pi\pi}\,(B^{+-}_{\pi\pi} - 2B^{+0}_{\pi\pi} - 2B^{00}_{\pi\pi})}{2B^{00}_{\pi\pi}\,(B^{+-}_{\pi\pi} + 2B^{+0}_{\pi\pi} - 2B^{00}_{\pi\pi})}. \tag{32}$$

There have also been attempts [29] to derive isospin bounds on $\cos(2\theta)$ in the $B^0_d \to \pi^+\pi^-$ decay which are based on the knowledge of the direct CP asymmetry $C^{+-}_{\pi\pi}$ alone. As for the GLSS bound [28], the starting point is the isospin-based triangular relation between the A^{+-}, A^{00} and A^{+0} amplitudes:

$$\frac{A^{+-}}{\sqrt{2}} + A^{00} = A^{+0}, \tag{33}$$

corresponding to the $B^0_d \to \pi^+\pi^-$, $B^0_d \to \pi^0\pi^0$ and $B^+ \to \pi^+\pi^0$ decays, respectively, and a similar one for the phase-shifted charged-conjugate amplitudes $\tilde{A}^{ij} = \mathrm{e}^{2i\gamma}\,\bar{A}^{ij}$. The graphical representation of both triangles is shown in Fig. 2. It should be noted that the magnitude of the difference between the A^{+-} and $\tilde{A}^{+-}$ amplitudes is $\sqrt{2}|P_c|\sin\gamma$ and not $\sqrt{2}|P_t|\sin\alpha$ as the c-convention [20] is employed for the amplitudes throughout this paper. With the help of the sine theorem, $\sin|2\theta|$ can be written as:

$$\sin|2\theta| = \frac{2|P_c|\sin\gamma}{|A^{+-}|}\sin\theta_A = \frac{2|P_c|\sin\gamma}{|\bar{A}^{+-}|}\sin\tilde{\theta}_A. \tag{34}$$

Squaring all the terms, the above relation can be rewritten as two inequalities:

$$\sin^2|2\theta| \leq 2\,\frac{1 - y^{+-}_{\pi\pi}\cos(2\theta)}{1 + C^{+-}_{\pi\pi}}, \qquad \sin^2|2\theta| \leq 2\,\frac{1 - y^{+-}_{\pi\pi}\cos(2\theta)}{1 - C^{+-}_{\pi\pi}}, \tag{35}$$

following from the conditions $\sin^2\theta_A \leq 1$ and $\sin^2\tilde{\theta}_A \leq 1$, respectively. Here, Eqs. (15), (16) and (24) were used to eliminate $|A^{+-}|^2$, $|\bar{A}^{+-}|^2$ and $|P_c|^2$. While $\sin^2|2\theta| \leq 1$, this does not imply that the expressions on the r.h.s. of (35) also satisfy this upper bound. Hence, no bound on $|2\theta|$ follows from Eq. (35)[f] and the GLSS bounds are indeed the strongest isospin-based bounds in the $B \to \pi\pi$ sector.

[f] We are grateful to David London and Nita and Rahul Sinha for pointing this out to us.

In addition to the above bounds on $\cos(2\theta)$, bounds on the CKM angle γ have also been derived in the literature recently which are based on the study of the correlation $\gamma - S^{+-}_{\pi\pi}$, given $\sin(2\beta)$ [30,31,19]. We reproduce these bounds below and discuss their impact in the next section. Relating the unitarity triangle angles β and γ with the Wolfenstein parameters $\bar\rho$ and $\bar\eta$:

$$1 - \bar\rho \pm i\bar\eta = R_t\, e^{\pm i\beta}, \qquad \bar\rho \pm i\bar\eta = R_b\, e^{\pm i\gamma}, \tag{36}$$

where R_t and R_b are defined in Eq. (2), the quantities $R^{+-}_{\pi\pi}$, $C^{+-}_{\pi\pi}$ and $S^{+-}_{\pi\pi}$ can be expressed in the form:

$$R^{+-}_{\pi\pi} = 1 + \frac{2\bar\rho}{R_b}\left|\frac{P_c}{T_c}\right|\cos\delta_c + \left|\frac{P_c}{T_c}\right|^2, \tag{37}$$

$$C^{+-}_{\pi\pi} = \frac{2\bar\eta}{R_b R^{+-}_{\pi\pi}}\left|\frac{P_c}{T_c}\right|\sin\delta_c, \tag{38}$$

$$S^{+-}_{\pi\pi} = \frac{-2\bar\eta}{R_b^2 R_t^2 R^{+-}_{\pi\pi}}\left[\bar\rho - R_b^2 + (1-R_b^2)R_b\left|\frac{P_c}{T_c}\right|\cos\delta_c + (1-\bar\rho)R_b^2\left|\frac{P_c}{T_c}\right|^2\right]. \tag{39}$$

The relation for $S^{+-}_{\pi\pi}$ given above agrees with Eq. (5) of the paper by Buchalla and Safir [30], if one introduces the pure strong-interaction quantity

$$r \equiv R_b\left|\frac{P_c}{T_c}\right|, \tag{40}$$

used by these authors. Note also that the equation for $C^{+-}_{\pi\pi}$ can be rewritten in terms of this quantity r in the following form:

$$(\bar\rho + r\cos\delta_c)^2 + \left(\bar\eta - \frac{r\sin\delta_c}{C^{+-}_{\pi\pi}}\right)^2 = \left(\frac{y^{+-}_{\pi\pi}}{C^{+-}_{\pi\pi}}\, r\sin\delta_c\right)^2. \tag{41}$$

For the phenomenological analysis, it is more convenient to eliminate $\bar\rho$ from Eqs. (38) and (39) with the help of the relation [30]:

$$1 - \bar\rho = \bar\eta\cot\beta \equiv \bar\eta\,\tau. \tag{42}$$

With this, the Wolfenstein parameter $\bar\eta$ can be related to either $S^{+-}_{\pi\pi}$ or $C^{+-}_{\pi\pi}$ as follows:

$$\bar\eta^{(S)} = \frac{1}{(1+\tau^2)S^{+-}_{\pi\pi}}\Big[(1+\tau\,S^{+-}_{\pi\pi})(1+r\cos\delta_c) \pm \sqrt{(1-S^{+-}_{\pi\pi})^2(1+r\cos\delta_c)^2 - (1+\tau^2)S^{+-}_{\pi\pi}\,[S^{+-}_{\pi\pi} + \sin(2\beta)]r^2\sin^2\delta_c}\Big], \tag{43}$$

$$\bar\eta^{(C)} = \frac{1}{2}(1+r\cos\delta_c)\sin(2\beta) + \frac{1}{(1+\tau^2)C^{+-}_{\pi\pi}}\Big[r\sin\delta_c \pm \sqrt{(1+\tau^2)(y^{+-}_{\pi\pi})^2 r^2\sin^2\delta_c - \left[C^{+-}_{\pi\pi}(1+r\cos\delta_c) - \tau\, r\sin\delta_c\right]^2}\Big]. \tag{44}$$

The first of these relations has been obtained by Buchalla and Safir (BS) [30], and has been used to derive an upper bound on $\bar\eta$ and, hence, a lower bound on γ:

$$\gamma \geq \frac{\pi}{2} - \arctan\frac{S^{+-}_{\pi\pi} - \tau\left[1 - \sqrt{1-(S^{+-}_{\pi\pi})^2}\right]}{1 + \tau S^{+-}_{\pi\pi} - \sqrt{1-(S^{+-}_{\pi\pi})^2}}, \tag{45}$$

which holds in the range $-\sin(2\beta) \leq S^{+-}_{\pi\pi} \leq 1$. However, the current central experimental value (7) of $S^{+-}_{\pi\pi}$ practically coincides with the central value (4) of $-\sin(2\beta)$, and hence no useful bound on the

CKM angle γ follows from the BS bound at present. We shall show this bound as a function of $S^{+-}_{\pi\pi}$, as well as its extension for the case of $C^{+-}_{\pi\pi} \neq 0$:

$$\tan\gamma \geq L_- = \frac{1 + S^{+-}_{\pi\pi}\sin(2\beta) + \sqrt{1-(C^{+-}_{\pi\pi})^2-(S^{+-}_{\pi\pi})^2}\cos(2\beta)}{\sqrt{1-(C^{+-}_{\pi\pi})^2-(S^{+-}_{\pi\pi})^2}\sin(2\beta) - S^{+-}_{\pi\pi}\cos(2\beta)}, \tag{46}$$

obtained by Botella and Silva [31]. The next step in the generalization of the BS bound was recently undertaken by Lavoura [19] who considered the modification of this bound by putting restrictions on the strong phase δ_c. With the current experimental values of $S^{+-}_{\pi\pi}$ and $C^{+-}_{\pi\pi}$, also the Botella-Silva and Lavoura versions of the BS bound are currently not useful in constraining γ. With precise measurements of $C^{+-}_{\pi\pi}$ and $S^{+-}_{\pi\pi}$ in future, these bounds may, in any case, provide useful consistency checks for the dynamical models used in the estimates of r and δ_c.

4 Numerical Analysis of the CP Asymmetry in $B^0_d \to \pi^+\pi^-$ Decay

Within the SM, the targets for the experiments measuring the angles α and γ are fairly well defined, as the fits of the unitarity triangle through the measurements of the CKM matrix elements yield the following ranges for these angles at 95% C.L. [25]:

$$70^\circ \leq \alpha \leq 115^\circ\ , \qquad 43^\circ \leq \gamma \leq 86^\circ\ . \tag{47}$$

The corresponding 95% C.L. ranges obtained using the default values of the input parameters by the CKM fitter group [24] are very similar:

$$77^\circ \leq \alpha \leq 122^\circ\ , \qquad 37^\circ \leq \gamma \leq 80^\circ\ . \tag{48}$$

So, if the SM is correct, and currently there is no experimental reason to believe otherwise, then from the $B \to \pi\pi$ analysis, values of α and γ should emerge which are compatible with their anticipated ranges listed above. Of course, the hope is that direct measurements of these angles will greatly reduce the currently allowed ranges. However, for this to happen, one has to determine the dynamical quantities $|P_c/T_c|$ and δ_c.

Surveying the recent literature on the estimates of $|P_c/T_c|$ and δ_c in $B \to \pi\pi$ decays, we remark that they are either based on specific schemes based on factorization in which non-factorizing effects are implemented using perturbative QCD in the large-m_b limit [33,34], or on phenomenological approaches based on some input from other data and factorization. A typical study in the latter case makes use of the data on the $B \to \pi\ell\nu_\ell$ and $B \to K\pi$ decays, which are used in conjunction with the assumption of factorization and estimates of the $SU(3)$-breaking effects [35]. Some representative estimates in these approaches are as follows: $|P_c/T_c| = 0.285 \pm 0.076$ [Beneke, Buchalla, Neubert, Sachrajda] [36], $|P_c/T_c| = 0.32^{+0.16}_{-0.09}$ [Beneke, Neubert] [37], $|P_c/T_c| = 0.29 \pm 0.09$ [Buchalla, Safir] [30], $|P_c/T_c| = 0.23^{+0.07}_{-0.05}$ [Keum, Sanda] [38], $|P_c/T_c| = 0.276 \pm 0.064$ [Gronau, Rosner] [7], $|P_c/T_c| = 0.26 \pm 0.08$ [Luo, Rosner] [35]. (See, also Xiao *et al.* [39]). Thus, $|P_c/T_c| = 0.30$ is a typical value from these estimates.

What concerns the strong phase difference δ_c, the two dynamical approaches developed in detail (QCD-Factorization [33] and pQCD [34]) differ considerably from each other due to a different power counting and the treatment of the annihilation contributions in the decay amplitudes. When comparing the current data with these specific approaches, we shall take for the sake of definiteness the estimates by Buchalla and Safir [30] to represent the QCD-factorization approach, $|P_c/T_c| = 0.29 \pm 0.09$ and $\delta_c = 0.15 \pm 0.25$ radians ($\delta_c = 9^\circ \pm 15^\circ$), and the estimates by Keum and Sanda [40], $|P_c/T_c| = 0.23^{+0.07}_{-0.05}$ and $-41^\circ \leq \delta_c \leq -32^\circ$, for the pQCD approach. Within the SM, the consistency test of these approaches lies in an adequate description of the data on $S^{+-}_{\pi\pi}$ and $C^{+-}_{\pi\pi}$, with the parameters α, γ, $|P_c/T_c|$ and δ_c all lying in their specified ranges. However, as $|P_c/T_c|$ and δ_c are not known directly from data or a first

principle calculation, we can leave them as free parameters and determine them from the overall fits. We shall pursue both approaches in this section.

We now present our numerical analysis of the current averages of $S^{+-}_{\pi\pi}$ and $C^{+-}_{\pi\pi}$ given in (7). For the construction of the C.L. contours, the following χ^2-function is used:

$$\chi^2 = \left[\frac{C^{+-}_{\pi\pi} - (C^{+-}_{\pi\pi})_{\rm exp}}{\Delta C^{+-}_{\pi\pi}}\right]^2 + \left[\frac{S^{+-}_{\pi\pi} - (S^{+-}_{\pi\pi})_{\rm exp}}{\Delta S^{+-}_{\pi\pi}}\right]^2 , \tag{49}$$

which is equated to 2.30, 6.18, and 11.83, corresponding to 68.3%, 95.5%, and 99.7% C.L., respectively, for two degrees of freedom.

We start by showing that the current data on $C^{+-}_{\pi\pi}$ and $S^{+-}_{\pi\pi}$ in the $B^0_d \to \pi^+\pi^-$ decays provides a discrimination among various dynamical approaches, for which the QCD factorization [33] and perturbative QCD [34] approaches will be taken as the two leading contenders. The results of this analysis are presented in Fig. 4 for six values of α in the range $80^\circ \le \alpha \le 130^\circ$ in intervals of 10°. To take into account the dispersion in the values of $|P_c/T_c|$, we take three values of this ratio, namely 0.30, 0.55, and 0.80. The first of these values represents the current expectations of this quantity, whereas the last is taken with the hindsight of the best fit of the data that we have performed in a model-independent way, as described later. The points indicated on these contours represent the values of the strong phase difference δ_c which is varied in the interval $-\pi \le \delta_c \le \pi$. We do not show the plot for $\alpha = 70^\circ$, which is the 95% C.L. lower value of α from the unitarity fits, as already the case $\alpha = 80^\circ$ requires rather large value of $|P_c/T_c|$. In each figure, the outer circle corresponds to the constraint $(S^{+-}_{\pi\pi})^2 + (C^{+-}_{\pi\pi})^2 = 1$. The current average (7) of the BABAR and BELLE data satisfies this constraint as shown by the data point with (unscaled) errors. The two ellipses surrounding the experimental measurement represent the 68.3% and 95.5% C.L. contours. This figure demonstrates that, as $C^{+-}_{\pi\pi}$ is negative and large, current data favors a rather large strong phase, typically $-60^\circ \le \delta_c \le -30^\circ$. The two shaded regions shown in this figure correspond to the predictions of the QCD-factorization approach (the upper shaded area) and the perturbative QCD framework (the lower shaded area). As can be seen, the predictions of the QCD-factorization approach lie outside of the 3σ experimental measurements for all values of α shown in this figure. For the perturbative QCD framework [34], one finds agreement with the measurements, but only at about 2σ level. Restricting α in the region $90^\circ \le \alpha \le 110^\circ$, good fits of the data are obtained for typically $|P_c/T_c| \ge 0.5$ and $\delta_c \le -30^\circ$. We shall quantify the fits more precisely later.

We now turn to a model-independent analysis of the $C^{+-}_{\pi\pi}$ and $S^{+-}_{\pi\pi}$ data. As the current world averages of these quantities are negative and rather large (7), positive values of the strong phase difference δ_c are excluded at a high confidence level ($> 99.7\%$ C.L.) which is demonstrated in Figs. 5, 6 and 7. This observation is the reason why the full range $-\pi \le \delta_c \le +\pi$ has been restricted to the negative values of δ_c, $-\pi \le \delta_c \le 0$, in these figures. In Fig. 5, three representative values (90°, 105° and 120°) of the angle α from the UT-favored interval (48) and three values (25.9°, 23.8° and 21.9°) of the angle β, which cover the present measurement of this quantity within $\pm 1\sigma$ range (4), are shown and the resulting χ^2-contours in the variables $|P_c/T_c|$ and δ_c are plotted. Note that the dependence on the precise value of β in the current experimental range of this angle is rather weak. Hence, we show the β-dependence of the correlation for only one value of α, namely $\alpha = 105^\circ$. The most important message from this analysis is that the current data favours negative and rather large values of the strong phase δ_c, which are correlated with the values of α. Restricting to the 68.3% C.L. contours for the sake of definiteness, the minimum allowed values of $-\delta_c$ are: 30°, 45°, and 70° for $\alpha = 90^\circ$, 105°, and 120°, respectively. What concerns the allowed values of $|P_c/T_c|$, we note that except for a relatively small allowed region near $80^\circ \le \alpha \le 90^\circ$, they overlap with the theoretical estimates of the same specified above at 95.5% C.L. However, the best-fit values of $|P_c/T_c|$ are on the higher side as shown by the dots in these figures. It should be noted that the current data results in the lower bound on the penguin-to-tree ratio $|P_c/T_c| \ge 0.18$ at 95.5% C.L but extends to much larger values of $|P_c/T_c|$, which we have suppressed in these figures for the sake of clarity but will show in the next section where we discuss the fits of the unitarity triangle.

The correlations between α and δ_c for three fixed values $|P_c/T_c| = 0.25$, 0.35, and 0.45 in the theoretically motivated interval are shown in Fig. 6. This figure updates the results by the BELLE

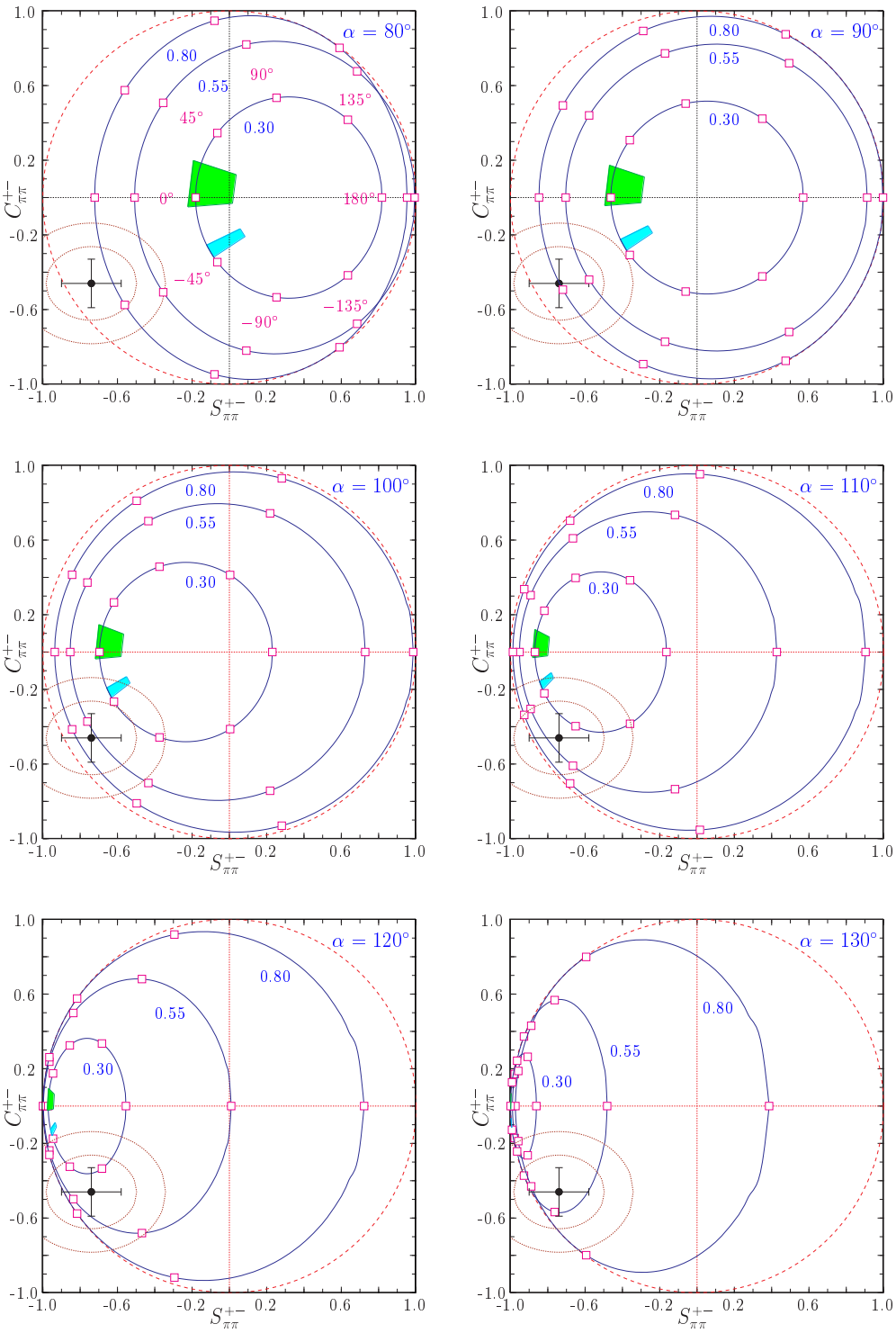

Figure 4. Implications of the time-dependent CP asymmetry parameters $C^{+-}_{\pi\pi} = -0.46 \pm 0.13$ and $S^{+-}_{\pi\pi} = -0.74 \pm 0.16$ from the BELLE and BABAR measurements for the CP violating phase α (or ϕ_2). In this analysis, the strong phase δ_c is varied over the full range $-\pi \leq \delta_c \leq \pi$ and curves are drawn for three values $|P_c/T_c| = 0.30$, 0.55, and 0.80. The predictions of the QCD factorization (upper box) and pQCD (lower box) approaches are also shown for fixed values of α noted on the six frames. The curves around the data point represent the 68.3% and 95.5% C.L. contours.

collaboration [10] and shows that a satisfactory description of the current data for these values of $|P_c/T_c|$ and with α lying within the indirect UT-based range is possible only with large values of the strong phase $-\delta_c$. Again using the 68.3% C.L. contours, it is seen that the minimum allowed value for $|P_c/T_c| = 0.35$ is $-\delta_c \simeq 55°$, and it decreases to 45° for $|P_c/T_c| = 0.45$. With $0.20 < |P_c/T_c| < 0.45$, the angles α and δ_c lie in the intervals: $90° \leq \alpha \leq 130°$ and $-160° \leq \delta_c \leq -30°$, at the 95.5% C.L. As higher values of $|P_c/T_c|$ are experimentally allowed, the correlations between α and δ_c for larger values of $|P_c/T_c| = 0.55$, 0.65, and 0.75 are shown in Fig. 7. We note that with these values, the allowed ranges for the angles α and δ_c become wider with increasing $|P_c/T_c|$.

The correlations between the angle α and $|P_c/T_c|$, for three representative values of the strong-phase difference $\delta_c = -40°$, $-80°$, and $-120°$ and the angle β within its experimental range, are presented in Fig. 8. This figure demonstrates again that smaller values of $|\delta_c|$ require larger values of $|P_c/T_c|$. The restrictions on $|P_c/T_c|$ and α discussed above are also seen in this figure.

In summary, we see that current data allows a wide range of the quantities $|P_c/T_c|$ and δ_c, and without restricting them the impact of the $C^{+-}_{\pi\pi}$ and $S^{+-}_{\pi\pi}$ measurements on the CKM parameters, in particular the angles α or γ, is rather small. The dynamical approaches discussed above are not a great help as they are not good fits of the data within the SM.

4.1 Constraints on $\cos(2\theta)$ *from bounds based on the isospin symmetry*

As discussed in the previous section, the penguin contribution in the $B^0_d \to \pi^+\pi^-$ decay can be parameterized by the angle 2θ. Having at hand the experimental range of $C^{+-}_{\pi\pi}$, it is of interest to work out numerically the dependence between the ratio $|P_c/T_c|$ and $\cos(2\theta)$, given by Eq. (26). The results of this analysis are presented in Fig. 9 for six values of γ in the range $25° \leq \alpha \leq 75°$ in intervals of 10°. The solid lines in all the frames correspond to the central experimental value of $C^{+-}_{\pi\pi}$ (7) while the dashed lines correspond to the $\pm 1\sigma$ values of this quantity. Due to the functional dependence (26) of r_c^2 on $\cos(2\theta - 2\gamma)$, there exists a sign ambiguity and there are two solutions depending on $\theta > 0$ and $\theta < 0$. We show both of these solutions and each frame in this figure contains two sets of curves where the upper and the lower ones correspond to $\theta > 0$ and $\theta < 0$, respectively. The isospin symmetry and the existing data on the $B \to \pi\pi$ decays allow to put restrictions on $\cos(2\theta)$. The GLSS lower bound (31) on $\cos(2\theta)$ is based on the $B \to \pi\pi$ branching ratios and $y^{+-}_{\pi\pi}$. The recent experimental data on the branching ratios and the B^+- and B^0-meson lifetime ratio [9]:

$$\begin{aligned}
\mathcal{B}(B^0_d \to \pi^+\pi^-) &= (4.55 \pm 0.44) \times 10^{-6}, \\
\mathcal{B}(B^+ \to \pi^+\pi^0) &= (5.27 \pm 0.79) \times 10^{-6}, \\
\mathcal{B}(B^0_d \to \pi^0\pi^0) &= (1.90 \pm 0.47) \times 10^{-6}, \\
\tau_{B^+}/\tau_{B^0} &= 1.086 \pm 0.017,
\end{aligned}$$

have been used in getting the conservative numerical bound: $\cos(2\theta) > -0.03$. This bound is shown as vertical dashed lines in all the frames in Fig. 9. It should be noted that if the central values of the data are used instead, the resulting GLSS bound is:

$$\cos(2\theta)\Big|_{\rm GLSS} > 0.27 \ , \tag{50}$$

which is shown as the solid vertical lines in Fig. 9. The shift is mainly due to the current uncertainties in the branching ratios for $B^0_d \to \pi^0\pi^0$ and $B^+ \to \pi^+\pi^0$. Our analysis shows that putting a lower bound on $\cos(2\theta)$, $|P_c/T_c|$ gets significantly constrained. It is seen that the branch with $\theta < 0$ results in smaller values for $|P_c/T_c|$, which are concentrated in a relatively narrow interval. However, as γ increases, this interval becomes wider. *A priori*, it is difficult to argue which of the two solutions $\theta > 0$ and $\theta < 0$ should be entertained. Hence, in the implementation of the isospin-based bound on $\cos(2\theta)$ in the unitarity fits, we shall allow the sign of θ to take either value.

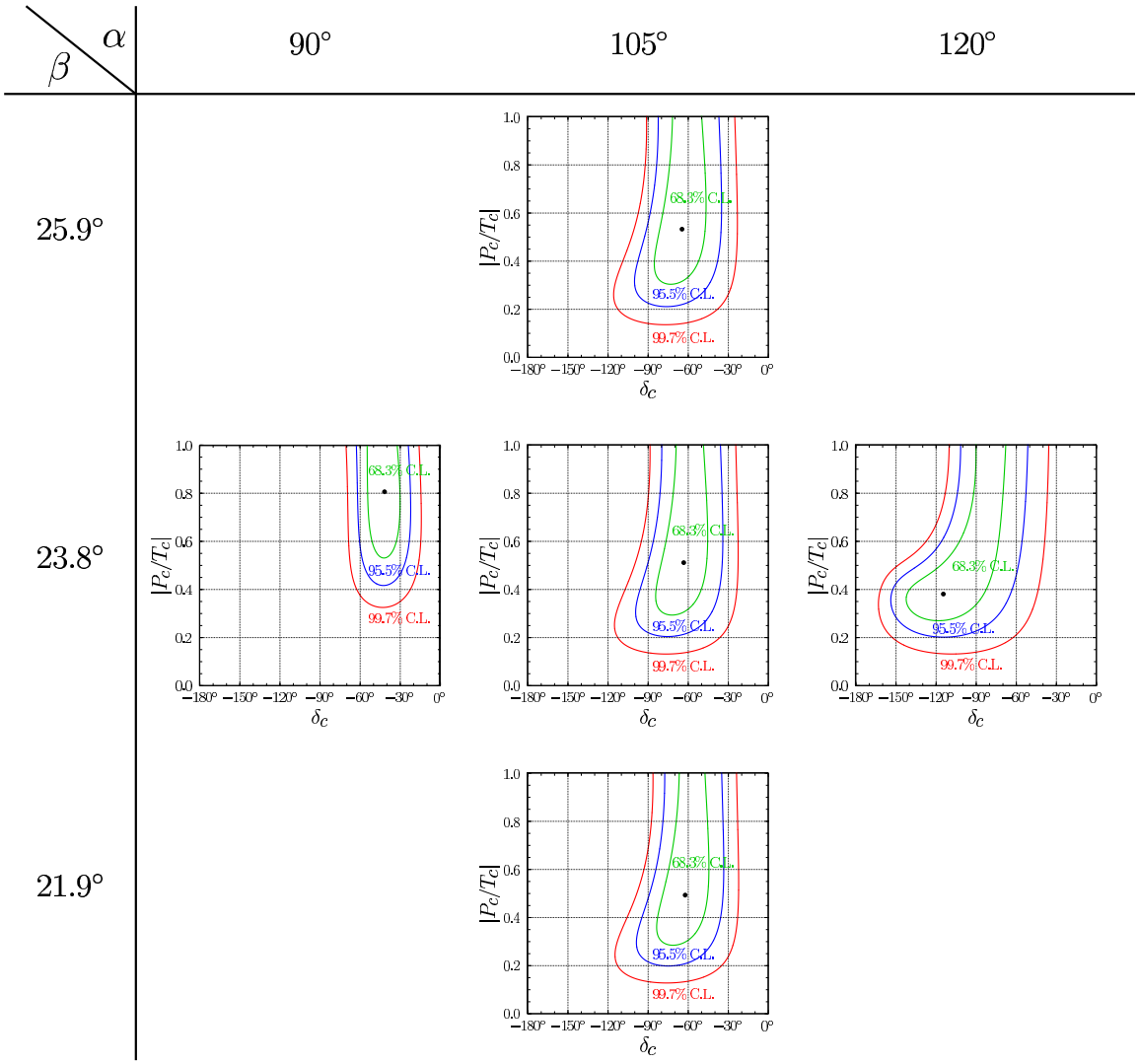

Figure 5. The correlation $|P_c/T_c| - \delta_c$ corresponding to the 68.3%, 95.5%, and 99.7% C.L. ranges of $C^{+-}_{\pi\pi}$ and $S^{+-}_{\pi\pi}$ for three values of α and β. Note that the dependence on β is rather weak and hence not shown for the other two values of α.

Based on the central values of the experimental data specified above and $C^{+-}_{\pi\pi}$ (7), the minimal value of the direct CP asymmetry in the $B^0_d \to \pi^0\pi^0$ decay (32) can be estimated as:

$$C^{00}_{\pi\pi} \geq 0.47. \tag{51}$$

It should be noted that $C^{00}_{\pi\pi}$ differs in sign from $C^{+-}_{\pi\pi}$. (See, also the recent analysis by Buras et al. [18].)

The SM-based bounds on the angle γ as a function of the CP asymmetry $S^{+-}_{\pi\pi}$ with $C^{+-}_{\pi\pi} = 0$ (the Buchalla-Safir bound [30]) and with $C^{+-}_{\pi\pi} = -0.46 \pm 0.13$ (the Botella-Silva bound [31]) are shown in Fig. 10 as the solid line and the shaded area, respectively. The vertical band corresponds to the current experimentally measured value, and the central value practically coincides with $S^{+-}_{\pi\pi} = -\sin(2\beta)$. Thus, these limits do not provide any restrictions on γ at present, but if with improved data a sizable shift of the $S^{+-}_{\pi\pi}$ central value from its current value takes place, then these bounds may lead to useful constraints.

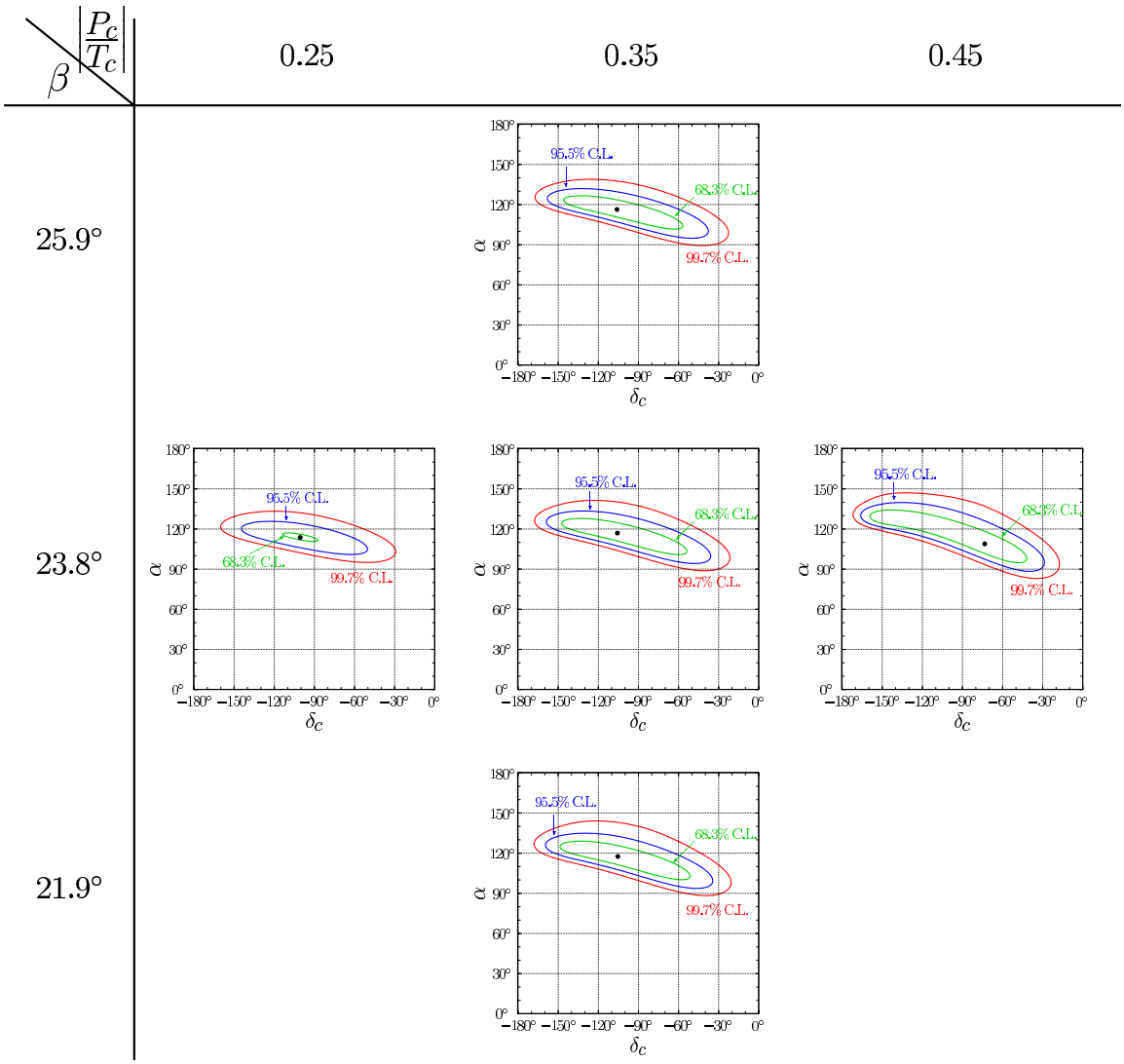

Figure 6. The correlation $\alpha - \delta_c$ corresponding to the 68.3%, 95.5%, and 99.7% C.L. ranges of $C^{+-}_{\pi\pi}$ and $S^{+-}_{\pi\pi}$ for $|P_c/T_c| =$ 0.25, 0.35, and 0.45.

5 Analysis of the CKM Unitarity Triangle Including $C^{+-}_{\pi\pi}$ and $S^{+-}_{\pi\pi}$ Measurements

In this section we investigate the impact of the $C^{+-}_{\pi\pi}$ and $S^{+-}_{\pi\pi}$ measurements on the unitarity triangle fits. We adopt a bayesian analysis method to fit the data. Systematic and statistical errors are combined in quadrature. We add a contribution to the chi-square for each of the inputs presented in Table 1. Other input quantities are taken from their central values given in the PDG review [41]. The lower bound on ΔM_{B_s} is implemented using the modified-χ^2 method (as described in the CERN CKM Workshop proceedings [42]), which makes use of the amplitude technique [43]. The $B_s \leftrightarrow \bar{B}_s$ oscillation probabilities are modified to have the dependence $P(B_s \to \bar{B}_s) \propto [1 + \mathcal{A}\cos(\Delta M_{B_s} t)]$ and $P(B_s \to B_s) \propto [1 -$

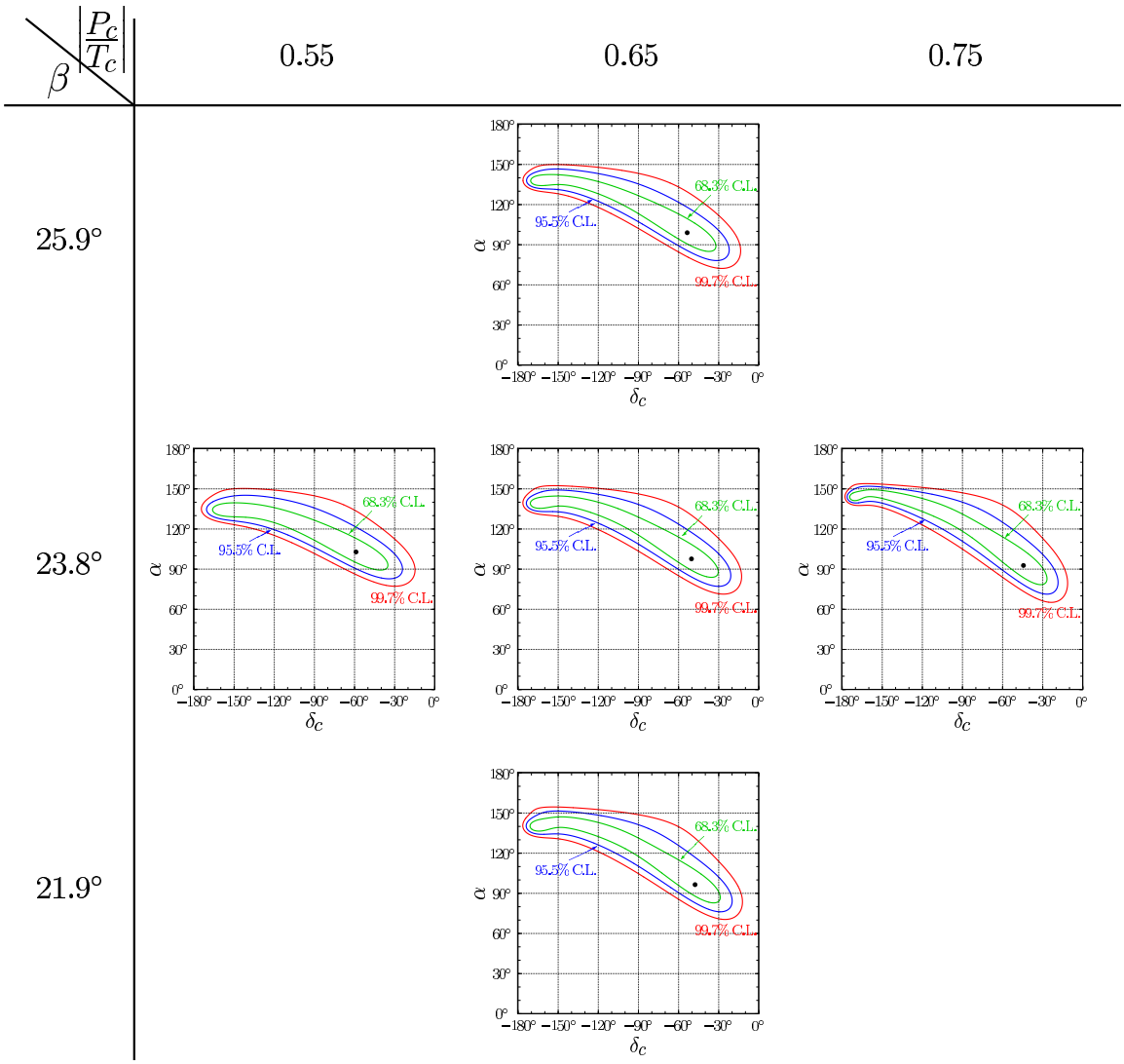

Figure 7. The correlation $\alpha - \delta_c$ corresponding to the 68.3%, 95.5%, and 99.7% C.L. ranges of $C_{\pi\pi}^{+-}$ and $S_{\pi\pi}^{+-}$ for $|P_c/T_c| = 0.55$, 0.65, and 0.75.

$\mathcal{A}\cos(\Delta M_{B_s} t)]$. The contribution to the χ^2-function is then

$$\chi^2(\Delta M_{B_s}) = 2\left[\mathrm{Erfc}^{-1}\left(\frac{1}{2}\,\mathrm{Erfc}\,\frac{1-\mathcal{A}}{\sqrt{2}\,\sigma_{\mathcal{A}}}\right)\right]^2 , \tag{52}$$

where $\mathcal{A}$ and $\sigma_{\mathcal{A}}$ are the world average amplitude and error, respectively. The measurements of $C_{\pi\pi}^{+-}$ and $S_{\pi\pi}^{+-}$ contribute to the χ^2-function according to Eq. (49). The resulting χ^2-function is then minimized over the following parameters: $\bar{\rho}$, $\bar{\eta}$, A, $\hat{B}_K$, η_1, η_2, η_3, $m_c(m_c)$, $m_t(m_t)$, η_B, $f_{B_d}\sqrt{B_{B_d}}$, ξ, $|P_c/T_c|$, and δ_c. Further details can be found in Ref. [25].

We present the output of the fits in Table 2, where we show the 68% C.L. ranges for the CKM parameters, the angles of the unitarity triangle, ΔM_{B_s}, $|P_c/T_c|$ and δ_c. Note the enormous ranges for $|P_c/T_c|$ and δ_c allowed by the UT fits. The 95% C.L. constraints from the five individual quantities (R_b, ϵ_K, ΔM_{B_d}, ΔM_{B_s}, and $a_{\psi K_S}$) and the resulting fit region (the shaded area) are shown in Fig. 11.

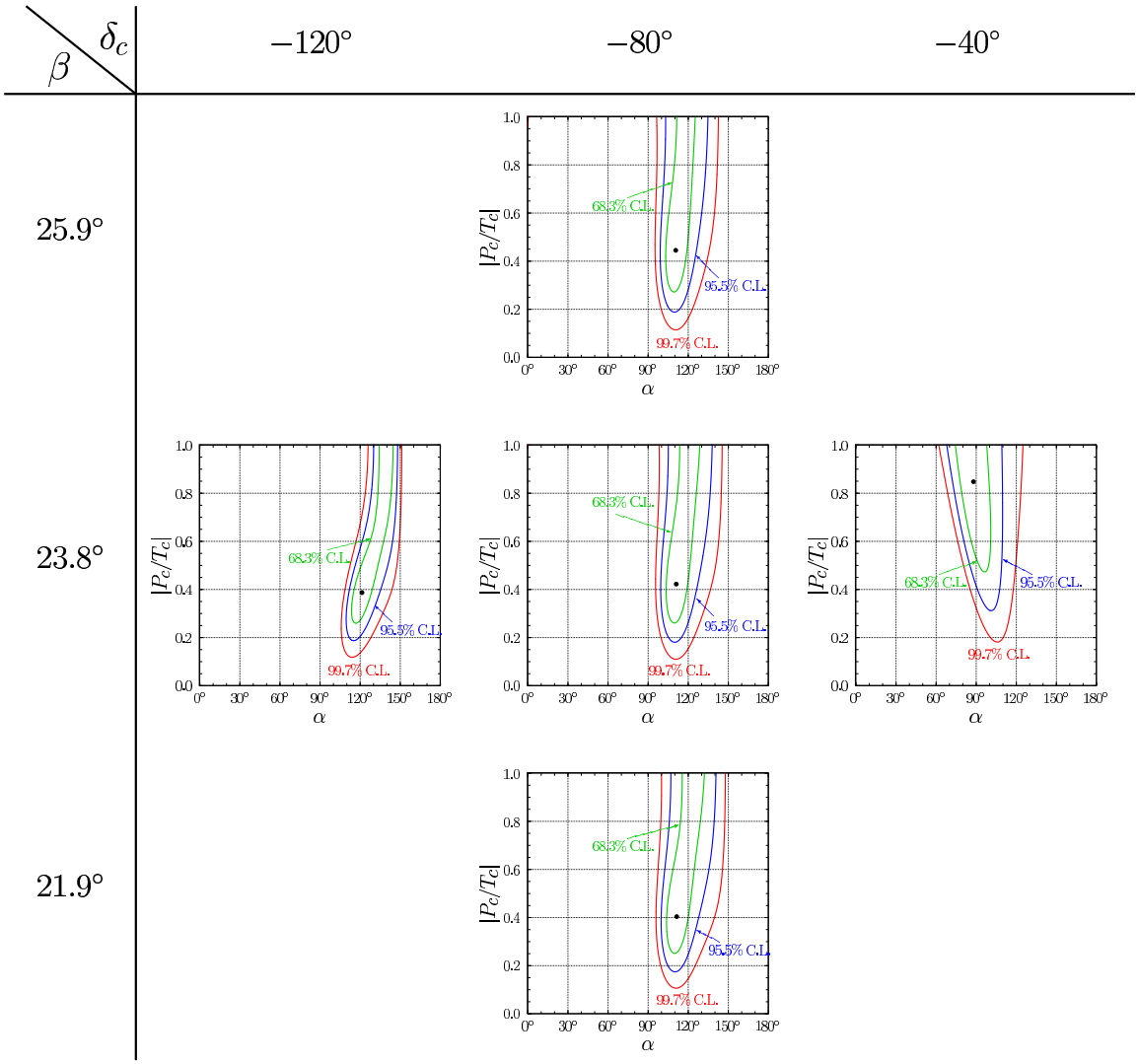

Figure 8. The correlation $|P_c/T_c| - \alpha$ corresponding to the 68.3%, 95.5%, and 99.7% C.L. ranges of $C^{+-}_{\pi\pi}$ and $S^{+-}_{\pi\pi}$ for $\delta_c = -120°$, $-80°$, and $-40°$.

Further details of this analysis and the discussion of the input parameters can be seen elsewhere [25]. The shaded areas in Fig. 12 are the 95% C.L. correlations between $\alpha - \gamma$ (the left frame) and $\sin(2\beta) - \sin(2\alpha)$ (the right frame). In Fig. 13 we show the behaviour of $\chi^2_{\rm min}$ as a function of the angle α (the dashed curve). The solid curves in all these figures will be explained below.

Note that the inclusion of the $C^{+-}_{\pi\pi}$ and $S^{+-}_{\pi\pi}$ measurements does not induce any additional constraint on the fits. This is because we added two additional terms to the χ^2-function with the dependence on two more variables $|P_c/T_c|$ and δ_c. Indeed, for any value of $\bar{\rho}$ and $\bar{\eta}$, it is always possible to choose $|P_c/T_c|$ and δ_c so as to exactly reproduce the $C^{+-}_{\pi\pi}$ and $S^{+-}_{\pi\pi}$ experimental central values. Thus, the total χ^2 of the unitarity triangle fit remains unchanged as the new measurements do not contribute to the total χ^2. In the two plots presented in Fig. 14 we fix $|P_c/T_c|$ (the left frame) and δ_c (the right frame) and minimize the χ^2-function with respect to all the other variables. In both cases, the absolute minimum of the curve coincides with the minimum χ^2 of the overall fit ($\chi^2_{\rm min} = 0.57$). A peculiar feature is the presence of two

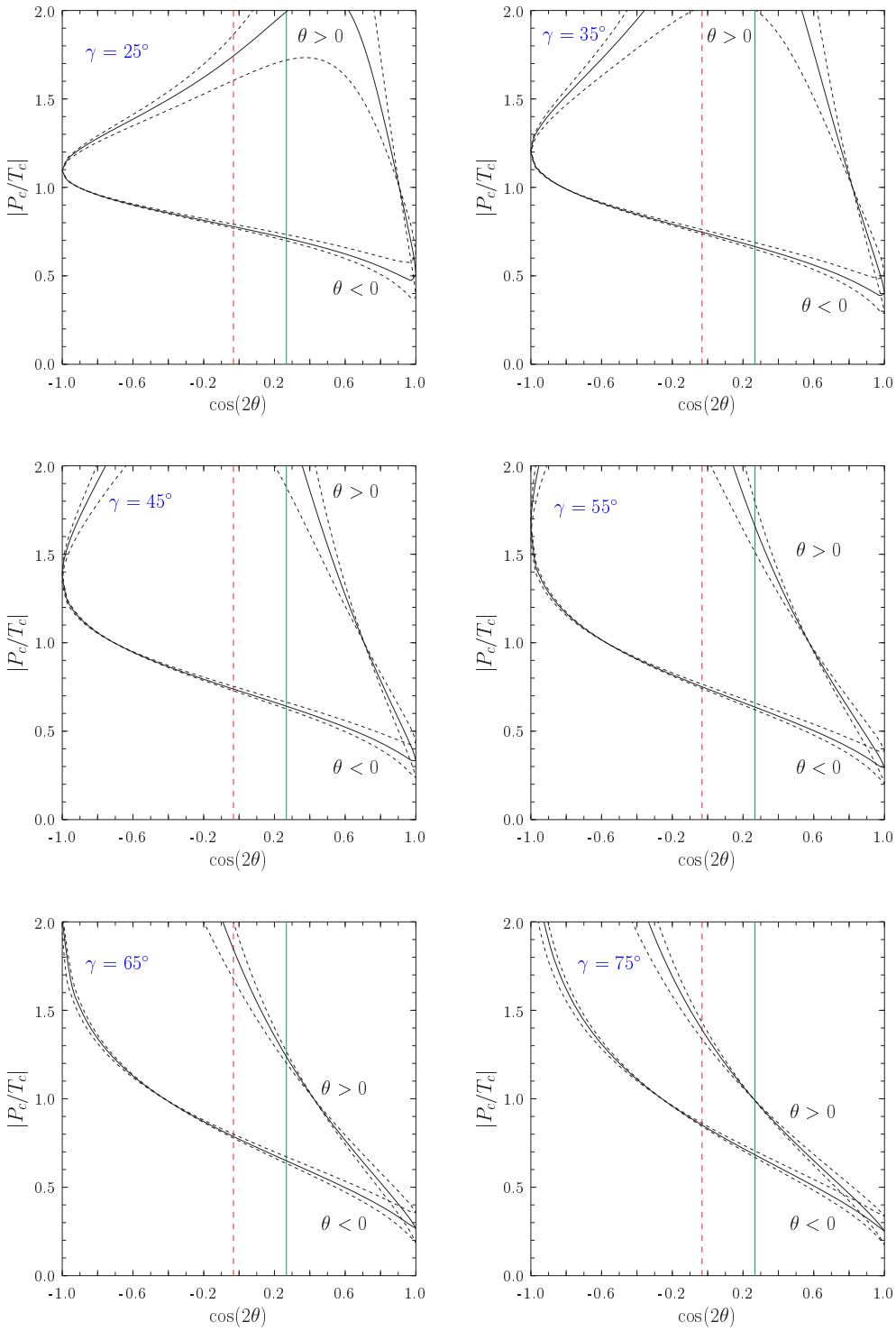

Figure 9. The correlation $|P_c/T_c| - \cos(2\theta)$ based on the current measurements of $C^{+-}_{\pi\pi}$ for fixed values of the angle γ indicated on the frames. The red dashed and green solid vertical lines represent the Gronau-London-Sinha-Sinha (GLSS) lower bounds $\cos(2\theta) > -0.03$ and $\cos(2\theta) > 0.27$, respectively, as discussed in the text. The upper and lower sets of curves correspond to the branches with $\theta > 0$ and $\theta < 0$, respectively.

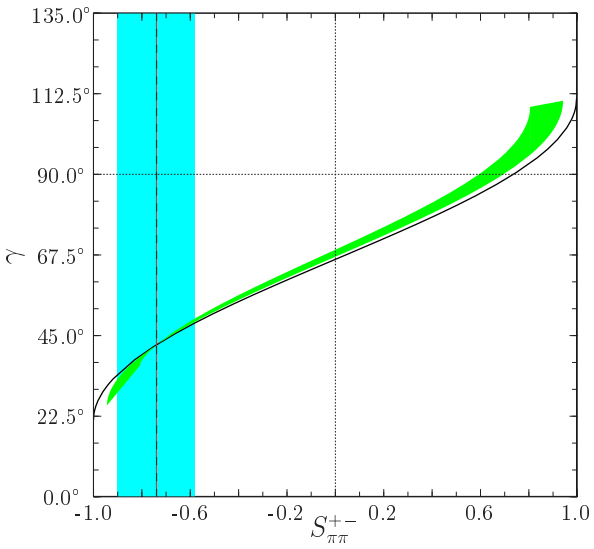

Figure 10. The SM limits on the angle γ in dependence on $S^{+-}_{\pi\pi}$ at $C^{+-}_{\pi\pi} = 0$ (the Buchalla-Safir limit) and at $C^{+-}_{\pi\pi} = -0.46 \pm 0.13$ (the Botella-Silva limit) shown as the solid line and the shaded area, respectively. Note that both are the lower limit for $S^{+-}_{\pi\pi} > -\sin(2\beta)$ and the upper one for $S^{+-}_{\pi\pi} < -\sin(2\beta)$. The vertical band corresponds to the experimentally measured value of $S^{+-}_{\pi\pi}$ with the recent central value which practically coincides with $S^{+-}_{\pi\pi} = -\sin(2\beta)$.

distinct regions for which the overall χ^2 is very small (the dashed curves). The best-fit values for $|P_c/T_c|$ and δ_c are $|P_c/T_c| = 0.77$ and $\delta_c = -43°$, respectively. Requiring higher confidence levels for the fits we obtain:

$$|P_c/T_c| \geq 0.23 \quad \& \quad \delta_c < -18° \quad @\,95\%\ \text{C.L.}, \tag{53}$$

$$|P_c/T_c| \geq 0.15 \quad \& \quad \delta_c < -13° \quad @\,99\%\ \text{C.L.}. \tag{54}$$

Up to now we have not considered the impact of the isospin-based bounds in the analysis of the $B \to \pi\pi$ data on the fits of the unitarity triangle. In future, the implementation of these bounds could take the form of the GLSS bound shown in Fig. 9 and the BS bound shown in Fig. 10. However, due to the proximity of $S^{+-}_{\pi\pi}$ and $-\sin(2\beta)$ with each other in the current data, we will concentrate on implementing the GLSS lower bound on $\cos(2\theta)$ resulting from the isospin-based analysis of the $B \to \pi\pi$ data presented in the previous section. A possible implementation of this bound could be undertaken by minimizing the χ^2-function and rejecting points for which $\cos(2\theta)$ lies below the allowed range. Taking $\cos(2\theta) > 0.27$, this analysis results in the black contours in Figs. 11 and 12. Note that a part of the 95% C.L. region is now excluded. The impact of the $\cos(2\theta)$ lower bound on the χ^2-fit for the angle α is shown through the solid curve in Fig. 13. This does not change the best-fit value of α but restricts the allowed range of α by a few degrees at 95% C.L. The impact of the $\cos(2\theta)$ lower bound on the fits of the unitarity triangle and the correlations $\alpha - \gamma$ and $\sin(2\alpha) - \sin(2\beta)$ is currently not great, but this will change with improved measurements leading to tighter constraints on $\cos(2\theta)$, and eventually its measurement. The effect of the lower bound on $\cos(2\theta)$ is, however, very significant for the allowed value of $|P_c/T_c|$ and δ_c. This is shown in Fig. 14 through the solid curves for $|P_c/T_c|$ (left frame) and δ_c (right frame). While the best-fit values of these parameters have not changed, the allowed regions are now drastically reduced. Thus, at 68% C.L., the allowed values are:

$$|P_c/T_c| = 0.77^{+0.58}_{-0.34}, \qquad \delta_c = (-43^{+14}_{-21})°. \tag{55}$$

Note that the resulting contours from the analysis of $S^{+-}_{\pi\pi}$ and $C^{+-}_{\pi\pi}$ do not rely on any model-dependent assumption. Our results in (55) can be compared with the analysis by Buras *et al.* [17], obtained in the SM

by restricting β and γ in the ranges $2\beta = (47 \pm 4)^\circ$ and $\gamma = (65 \pm 7)^\circ$, which yields $|P_c/T_c| = 0.49^{+0.33}_{-0.21}$ and $\delta_c = (-43^{+19}_{-23})^\circ$. The two analyses are compatible with each other though they differ in the details, in how the exact isospin-relations were imposed in the analysis of the data (and also somewhat in the input data). However, we note that we have not restricted γ to any range, as it is a fit parameter returned by the unitarity fits, but our fit value $\gamma = (64 \pm 10)^\circ$ is compatible with the input value used by Buras *et al.* [17].

Finally, to show the impact of the $\cos(2\theta)$ bound on the unitarity triangle in a Gedanken experiment where the quantities $S^{+-}_{\pi\pi}$ and $C^{+-}_{\pi\pi}$ are assumed to be very precisely measured, we fix $S^{+-}_{\pi\pi}$ and $C^{+-}_{\pi\pi}$ to their current experimental central values (7) and show the allowed region in Fig. 15 resulting from the lower bound $\cos(2\theta) > 0.25$ (the shaded region). Note that this results in a constraint in the $\bar{\rho} - \bar{\eta}$ plane which is very similar to what one gets using a range for α. Since the experiments do not measure α, but rather $S^{+-}_{\pi\pi}$ and $C^{+-}_{\pi\pi}$, this figure shows how the eventual $S^{+-}_{\pi\pi}$ and $C^{+-}_{\pi\pi}$ measurements together with the lower bound on $\cos(2\theta)$ gets translated. This represents the strongest possible constraint on the profile of the unitarity triangle from the $S^{+-}_{\pi\pi}$ and $C^{+-}_{\pi\pi}$ measurements that one can get in a model-independent way. Of course, this figure itself is only illustrative, as the actual constraints will depend on the values of $S^{+-}_{\pi\pi}$ and $C^{+-}_{\pi\pi}$ and the lower bound on $\cos(2\theta)$ that will be eventually measured.

λ	0.2224 ± 0.002 (fixed)
$\lvert V_{cb}\rvert$	$(41.2 \pm 2.1) \times 10^{-3}$
$\lvert V_{ub}\rvert$	$(3.90 \pm 0.55) \times 10^{-3}$
$a_{\psi K_S}$	0.736 ± 0.049
$\lvert\epsilon_K\rvert$	$(2.280 \pm 0.13) \times 10^{-3}$
ΔM_{B_d}	(0.503 ± 0.006) ps^{-1}
$\eta_1(m_c(m_c) = 1.30$ GeV)	1.32 ± 0.32
η_2	0.57 ± 0.01
η_3	0.47 ± 0.05
$m_c(m_c)$	(1.25 ± 0.10) GeV
$m_t(m_t)$	(165 ± 5) GeV
$\hat{B}_K$	0.86 ± 0.15
$f_{B_d}\sqrt{B_{B_d}}$	$(215 \pm 11 \pm 15^{+0}_{-23})$ MeV
η_B	0.55 ± 0.01
ξ	$1.14 \pm 0.03 \pm 0.02^{+0.13+0.03}_{-0.0\ -0.0}$
ΔM_{B_s}	> 14.4 ps^{-1} at 95% C.L.

Table 1. The input parameters used in the CKM-unitarity fits. Their explanation and discussion can be found, for example, in Ref. 25.

6 Summary and Concluding Remarks

We have investigated the impact of the current measurements of the time-dependent CP-asymmetry parameters $S^{+-}_{\pi\pi}$ and $C^{+-}_{\pi\pi}$ in the $B^0_d/\bar{B}^0_d \to \pi^+\pi^-$ decays, reported by the BELLE and BABAR collaborations, on the CKM parameters. The results of our analysis can be summarized as follows.

In the first part of our analysis, we have compared the resulting world average (7) of these measurements with the predictions of the specific dynamical approaches [33,34] in which the quantities $|P_c/T_c|$ and δ_c are estimated. We find that, within the SM, they do not provide a good fit of the data. In particular, the estimates of $|P_c/T_c|$ and δ_c [30] based on the QCD factorization [33] are off the mark by more than 3 sigma. This was shown in Fig. 4 for a large enough range of the angle α. The mismatch between the data and the QCD-factorization approach [33] can also be studied by calculating the χ^2-function of

$\bar{\rho}$	$0.10 \div 0.24$
$\bar{\eta}$	$0.32 \div 0.40$
A	$0.79 \div 0.86$
$\sin(2\alpha)$	$-0.44 \div +0.30$
$\sin(2\beta)$	$0.69 \div 0.78$
$\sin(2\gamma)$	$0.50 \div 0.96$
α	$(81 \div 103)^\circ$
β	$(21.9 \div 25.5)^\circ$
γ	$(54 \div 75)^\circ$
ΔM_{B_s}	$(16.6 \div 20.3)$ ps^{-1}
$\lvert P_c/T_c \rvert$	$0.43 \div 5.3$
δ_c	$(-112 \div -29)^\circ$

Table 2. The 68% C.L. ranges for the CKM-Wolfenstein parameters, CP-violating phases, ΔM_{B_s}, $|P_c/T_c|$ and δ_c from the CKM-unitarity fits.

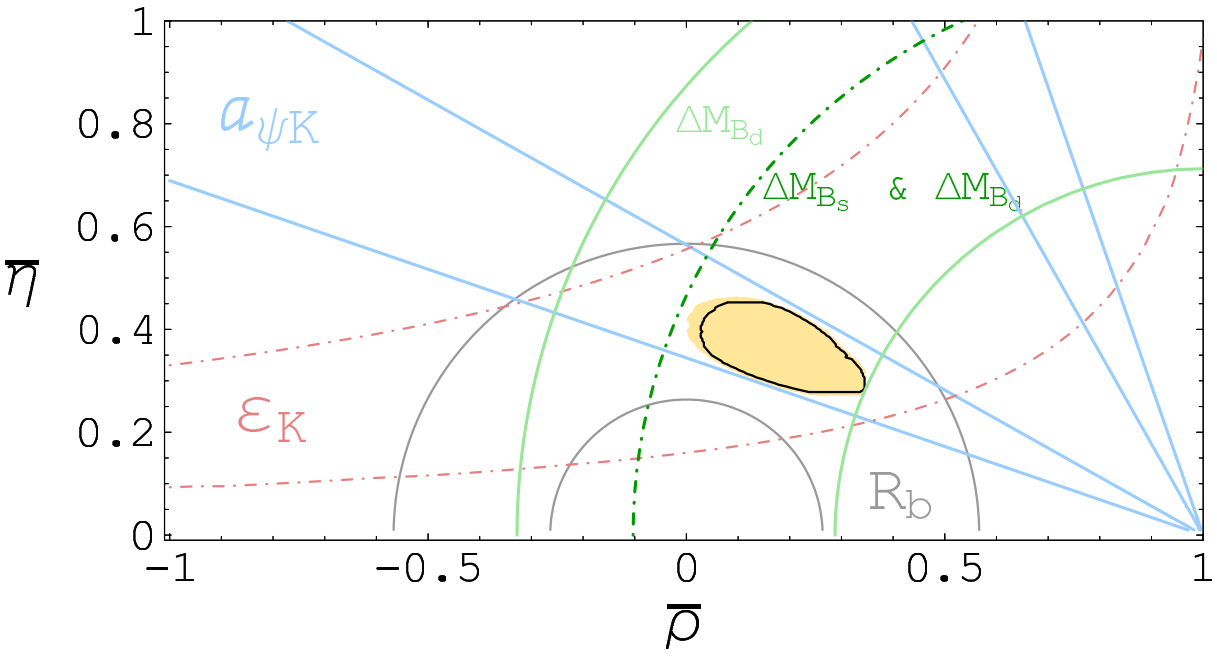

Figure 11. Constraints in the $\bar{\rho} - \bar{\eta}$ plane from the five measurements as indicated. Note that the curve labelled as ΔM_{B_s} is obtained from its 95% C.L. lower limit 14.4 ps^{-1}. The fit contour corresponds to 95% C.L. and the dot shows the best-fit value. The black contour shows the impact of the GLSS lower bound $\cos(2\theta) > 0.27$ resulting from the $C^{+-}_{\pi\pi}$ and $B \to \pi\pi$ branching ratios measurements and using the isospin symmetry.

the unitarity triangle fit with the estimates by Buchalla and Safir [30] for $|P_c/T_c|$ and δ_c as an input. The χ^2-minimum of the resulting fit is about 11 (compared to $\chi^2_{\rm min} = 0.57$, leaving these two parameters free), which corresponds to a probability of about 1%. Looking more closely to localize the source of this discrepancy, our fits show that it is the small value of the strong phase difference predicted in the QCD-factorization approach ($-6^\circ < \delta_c < 24^\circ$ at 68% C.L.) which should be compared to the fit of the

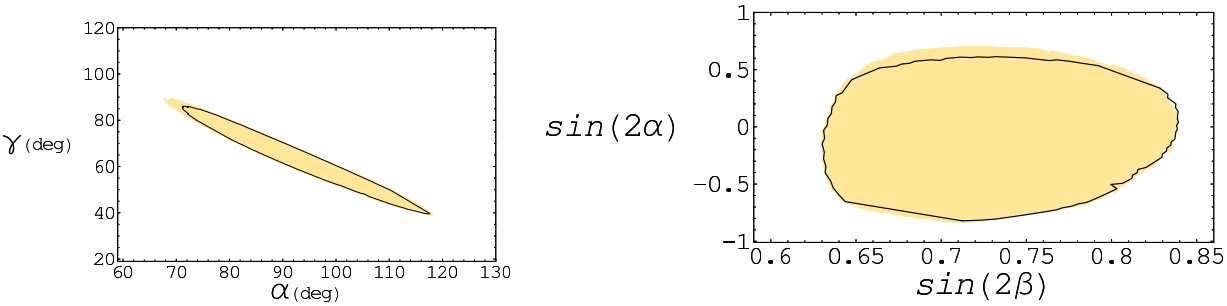

Figure 12. The 95% C.L. correlations between $\alpha - \gamma$ and $\sin(2\alpha) - \sin(2\beta)$ in the SM. The black contours show the impact of the GLSS lower bound $\cos(2\theta) > 0.27$ resulting from the $C^{+-}_{\pi\pi}$ and $B \to \pi\pi$ branching ratios measurements and using the isospin symmetry.

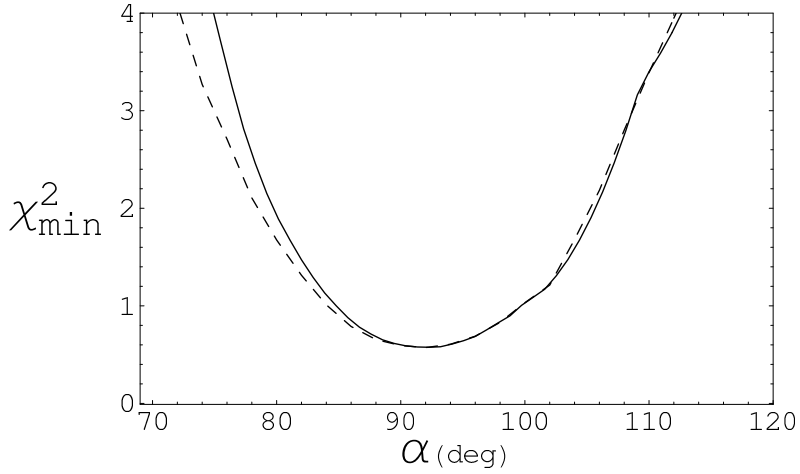

Figure 13. The $\chi^2_{\rm min}$-distribution as a function of the angle α from the unitarity fits of the CKM parameters in the SM including the current measurements of $C^{+-}_{\pi\pi}$ and $S^{+-}_{\pi\pi}$. The dashed (solid) curve is obtained without (with) taking into account the lower bound $\cos(2\theta) > 0.27$.

data obtained by leaving the two parameters free, yielding $-64° < \delta_c < -29°$, which contributes mainly to the chi square and hence results in the poor quality of the fit. Since a similar inference also follows for the CP asymmetry $\mathcal{A}_{\rm CP}(K^+\pi^-)$ in the $B^0_d \to K^+\pi^-$ decay, where the current measurements yield [8] $(-9.5 \pm 2.9)\%$, compared to the QCD-factorization prediction [37] $(+5 \pm 10)\%$, one must conclude, unless data change drastically, that this approach grossly underestimates the strong interaction phases in the $B \to \pi\pi$ and $B \to K\pi$ decays. The competing pQCD approach [34] fares comparatively somewhat better but predicts a smaller value of $|P_c/T_c|$ than is required by the current data. The central value of this quantity in the estimate by Keum and Sanda [38], $|P_c/T_c| = 0.23$, is approximately a factor of two smaller than the lowest value of this quantity from the fit range $0.43 \le |P_c/T_c| \le 1.35$ at 68% C.L., with the best-fit value being $|P_c/T_c| = 0.77$. The main message that comes out from this part of the analysis is that the QCD-penguin contributions are significantly stronger than most of their current phenomenological estimates, and it remains a theoretical challenge to understand this feature of the data.

In the second, and larger part of this paper, we have addressed the question of how to interpret the measurements of $S^{+-}_{\pi\pi}$ and $C^{+-}_{\pi\pi}$ in terms of the CKM parameters in a model-independent way. We find that leaving the dynamical quantities $|P_c/T_c|$ and δ_c as free parameters, the CKM unitarity fits do not effectively constrain these parameters, yielding a very large range even at 68% C.L. As a result of

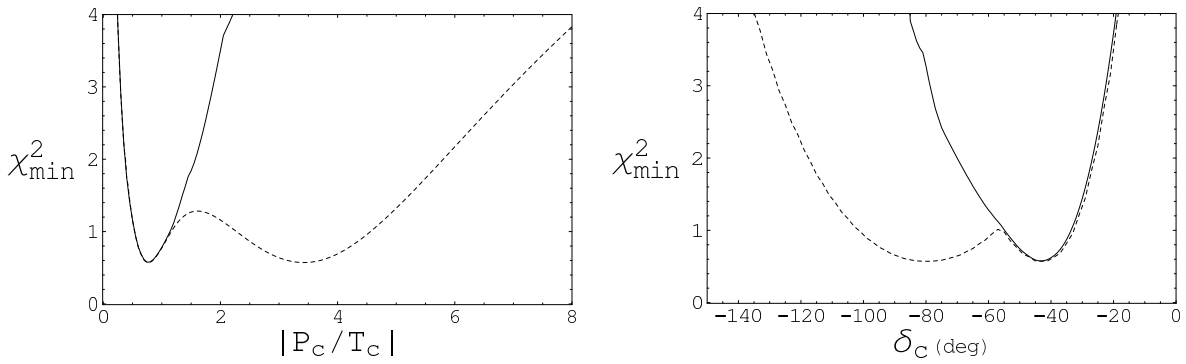

Figure 14. The $\chi^2_{\rm min}$-distributions as a function of $|P_c/T_c|$ (left frame) and the strong phase difference δ_c (right frame) from the unitarity fits of the CKM parameters in the SM including the current measurements of $C^{+-}_{\pi\pi}$ and $S^{+-}_{\pi\pi}$. The dashed (solid) curve is obtained without (with) taking into account the lower bound $\cos(2\theta) > 0.27$.

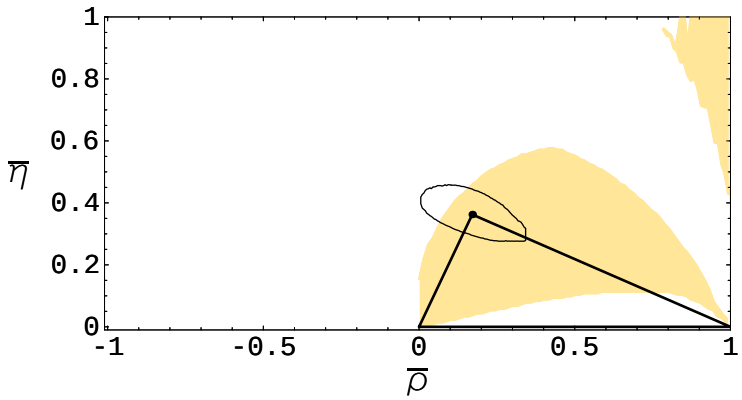

Figure 15. Constraints in the $\bar\rho - \bar\eta$ plane from the assumed exact measurements of $C^{+-}_{\pi\pi} = -0.46$ and $S^{+-}_{\pi\pi} = -0.74$ and the lower bound $\cos(2\theta) > 0.27$ (the shaded regions). The fit contour corresponds to the 95% C.L. unitarity fits without taking into account the $C^{+-}_{\pi\pi}$ and $S^{+-}_{\pi\pi}$ measurements.

this, the measurements of $S^{+-}_{\pi\pi}$ and $C^{+-}_{\pi\pi}$ have practically very little impact on the unitarity fits of the CKM-Wolfenstein parameters $\bar\rho$ and $\bar\eta$, and hence on the allowed values of the angles α and γ, unless these dynamical quantities are bounded. We have reviewed a number of proposals in the literature to put isospin-based bounds on the QCD-penguin contribution in the $B \to \pi\pi$ decays. Parameterizing it in terms of the angle 2θ, introduced by Grossman and Quinn, we find that the GLSS lower bound on $\cos(2\theta)$ is the strongest bound to date, which we have evaluated as $\cos(2\theta) > -0.03$ (propagating the errors on the input quantities) and as $\cos(2\theta) > 0.27$ (for the central values). We have worked out the consequences of the lower bound $\cos(2\theta) > 0.27$ on the profile of the unitarity triangle and the angles α and γ. Including the isospin-based constraint, our best fit values yield: $\alpha = 92°$, $\beta = 24°$ and $\gamma = 64°$, with the 68% C.L. ranges given in Table 2. The corresponding best-fit values of the dynamical parameters are found to be $|P_c/T_c| = 0.77$ and $\delta_c = -43°$, respectively, with their 68% C.L. ranges given in Eq. (55). With improved data expected in the near future, these ranges can be reduced significantly, leading to a precise determination of all three angles α, β and γ of the unitarity triangle.

Of course, at some stage, one has to take into account the isospin-breaking corrections. They originate, in part, from the electroweak penguins which are estimated to be numerically small [44,45,46], and this estimate can be put on model-independent grounds [47,48]. Moreover, they do not change the bounds obtained above for which the closure of the two triangles shown in Fig. 2 was used. However, the isospin-

breaking corrections may be significant from the $\pi^0 - \eta - \eta'$ mixing [49], in the presence of which the two isospin triangles used in our analysis do not close [50], leading to quadrilaterals. These latter corrections will have to be accounted for in the final determination of the angle α. As the current estimates of these corrections are model-dependent [50], we can not assign at present a quantitative weight to them. They will be better determined as and when the individual $B^0_d \to \pi^0\pi^0$ and $\bar{B}^0_d \to \pi^0\pi^0$ branching ratios are measured to which we look forward in the future.

Acknowledgements

We thank James Smith and Andreas Höcker for their help with the averaging of the current data on $C^{+-}_{\pi\pi}$ and $S^{+-}_{\pi\pi}$. One of us (A.A.) would also like to thank Masashi Hazumi for helpful discussions about the BELLE data. We are very grateful to David London, Nita and Rahul Sinha for pointing out our error in deriving a spurious isospin bound in the earlier version of this paper. Helpful communications from Andrzej Buras, Robert Fleischer and Dan Pirjol are also thankfully acknowledged. This work is partially supported by the KEK Directorate under a grant from the Japanese Ministry of Education, Culture, Sports, Science and Technology. E.L. and A.Ya.P. acknowledge financial support from the Schweizerischer Nationalfonds.

References

1. M. Kobayashi and T. Maskawa, Prog. Theor. Phys. **49** (1973) 652.
2. N. Cabibbo, Phys. Rev. Lett. **10** (1963) 531.
3. L. Wolfenstein, Phys. Rev. Lett. **51**, 1945 (1983).
4. A. J. Buras, M. E. Lautenbacher and G. Ostermaier, Phys. Rev. D **50**, 3433 (1994) [hep-ph/9403384].
5. T. Browder, hep-ex/0312024; To appear in the Proceedings of the XXI International Symposium on Lepton and Photon Interactions, Fermilab, Batavia, USA, 11 - 16 August 2003.
6. H. Jawahery, in the Proceedings of the XXI International Symposium on Lepton and Photon Interactions, Fermilab, Batavia, USA, 11 - 16 August 2003.
7. M. Gronau and D. London, Phys. Rev. Lett. **65**, 3381 (1990).
8. J. Fry, in the Proceedings of the XXI International Symposium on Lepton and Photon Interactions, Fermilab, Batavia, USA, 11 - 16 August 2003.
9. Heavy Flavor Averaging Group [HFAG]: http://www.slac.stanford.edu/xorg/hfag/.
10. K. Abe *et al.* [Belle Collaboration], Phys. Rev. D **68**, 012001 (2003) [hep-ex/0301032].
11. B. Aubert *et al.* [BABAR Collaboration], Phys. Rev. Lett. **89** (2002) 281802 [hep-ex/0207055].
12. K. Abe *et al.* [Belle Collaboration] hep-ex/0401029.
13. R. Fleischer, Eur. Phys. J. C **16**, 87 (2000) [hep-ph/0001253].
14. M. Gronau and J. L. Rosner, Phys. Rev. D **65**, 093012 (2002) [hep-ph/0202170].
15. R. Fleischer and J. Matias, Phys. Rev. D **66**, 054009 (2002) [hep-ph/0204101].
16. R. Fleischer, G. Isidori and J. Matias, JHEP **0305**, 053 (2003) [hep-ph/0302229].
17. A. J. Buras, R. Fleischer, S. Recksiegel and F. Schwab, Phys. Rev. Lett. **92**, 101804 (2004) [hep-ph/0312259].
18. A. J. Buras, R. Fleischer, S. Recksiegel and F. Schwab, hep-ph/0402112.
19. L. Lavoura, hep-ph/0402181.
20. M. Gronau and J. L. Rosner, Phys. Rev. D **66**, 053003 (2002) [Erratum-ibid. D **66**, 119901 (2002)] [hep-ph/0205323].
21. A. J. Buras and R. Fleischer, Phys. Lett. B **341**, 379 (1995) [hep-ph/9409244].
22. D. London, N. Sinha and R. Sinha, Phys. Rev. D **60**, 074020 (1999) [hep-ph/9905404].
23. G. C. Branco, L. Lavoura and J. P. Silva, *CP Violation* (Oxford Science Publications) (1999), p. 404.
24. A. Höcker, H. Lacker, S. Laplace and F. Le Diberder, Eur. Phys. J. C **21**, 225 (2001)

[hep-ph/0104062], CKMFitter Working Group, http://www.ckmfitter.in2p3.fr.
25. A. Ali, KEK-Preprint 2003-106, [hep-ph/0312303].
26. Y. Grossman and H. R. Quinn, Phys. Rev. D **58**, 017504 (1998) [hep-ph/9712306].
27. J. Charles, Phys. Rev. D **59** (1999) 054007 [hep-ph/9806468].
28. M. Gronau, D. London, N. Sinha and R. Sinha, Phys. Lett. B **514**, 315 (2001) [hep-ph/0105308].
29. A. K. Giri and R. Mohanta, hep-ph/0207249.
30. G. Buchalla and A. S. Safir, hep-ph/0310218.
31. F. J. Botella and J. P. Silva, hep-ph/0312337.
32. See, for example, the review by H. Quinn and A.I. Sanda in the Particle Data Group Listings [41].
33. M. Beneke, G. Buchalla, M. Neubert and C. T. Sachrajda, Phys. Rev. Lett. **83**, 1914 (1999) [hep-ph/9905312].
34. Y. Y. Keum, H. n. Li and A. I. Sanda, Phys. Lett. B **504**, 6 (2001) [hep-ph/0004004].
35. Z. Luo and J. L. Rosner, Phys. Rev. D **68**, 074010 (2003) [hep-ph/0305262].
36. M. Beneke, G. Buchalla, M. Neubert and C. T. Sachrajda, Nucl. Phys. B **606**, 245 (2001) [hep-ph/0104110].
37. M. Beneke and M. Neubert, Nucl. Phys. B **675**, 333 (2003) [hep-ph/0308039].
38. Y. Y. Keum and A. I. Sanda, Phys. Rev. D **67** (2003) 054009 [hep-ph/0209014].
39. For a survey of literature on the ratio $|P_c/T_c|$ and analysis of $B \to \pi\pi$, $K\pi$ data, see Z. j. Xiao, C. D. Lu and L. Guo, [hep-ph/0303070].
40. Y. Y. Keum and A. I. Sanda, eConf **C0304052**, WG420 (2003) [hep-ph/0306004].
41. K. Hagiwara *et al.* [Particle Data Group Collaboration], Phys. Rev. D **66**, 010001 (2002).
42. M. Battaglia *et al.*, hep-ph/0304132.
43. H. G. Moser and A. Roussarie, Nucl. Instrum. Meth. A **384**, 491 (1997).
44. N. G. Deshpande and X. G. He, Phys. Rev. Lett. **74**, 26 (1995) [Erratum-ibid. **74**, 4099 (1995)] [hep-ph/9408404].
45. M. Gronau, O. F. Hernandez, D. London and J. L. Rosner, Phys. Rev. D **52**, 6374 (1995) [hep-ph/9504327].
46. R. Fleischer, Phys. Lett. B **365**, 399 (1996) [hep-ph/9509204].
47. A. J. Buras and R. Fleischer, Eur. Phys. J. C **11**, 93 (1999) [hep-ph/9810260].
48. M. Gronau, D. Pirjol and T. M. Yan, Phys. Rev. D **60**, 034021 (1999) [hep-ph/9810482].
49. H. Leutwyler, Phys. Lett. B **374**, 181 (1996) [hep-ph/9601236].
50. S. Gardner, Phys. Rev. D **59**, 077502 (1999) [hep-ph/9806423].